Fall 12-21-2019

Peroxiredoxin 6 and Inflammation in Alzheimer's Disease

Jared Ferrell-Penniman
Southern Methodist University, jferrellpenniman@smu.edu

PEROXIREDOXIN 6 AND INFLAMMATION

IN ALZHEIMER'S DISEASE

Approved by:

Dr. William Orr
Department Chair and
Professor of Biological Sciences

Dr. Adam Norris
Assistant Professor of Biological Sciences

Dr. Svetlana Radyuk
Associate Professor of Biological Sciences

Dr. Pia Vogel
Professor of Biological Sciences

PEROXIREDOXIN 6 AND INFLAMMATION IN ALZHEIMER'S DISEASE

A Thesis Presented to the Graduate Faculty of

Dedman College

Southern Methodist University

In

Partial Fulfillment of the Requirements

for the degree of

Master of Science

In

Molecular and Cellular Biology

By

Jared Ferrell-Penniman

B.S., Biology, University of North Texas

December 21, 2019

Ferrell-Penniman, Jared B.S., Biology, University of North Texas

Peroxiredoxin 6 and Inflammation
in Alzheimer's Disease

Advisor: Professor William Orr
Master of Science conferred December 21, 2019
Thesis completed December 12, 2019

Alzheimer's disease (AD) is known for its debilitating symptoms and poor prognosis. Current treatments for AD focus on managing symptoms. However, despite intense research into neurodegenerative diseases, there is still a dearth of therapies targeted at the underlying mechanisms of the disease. Oxidative stress (OS) and inflammation are cellular phenomena thought to be key to the progression of the disease. Critically, peroxiredoxin 6 (Prx6), an antioxidant protein with multiple functions, has been identified from mammalian studies as a potential regulator of both OS and inflammation that may have a specific effect on AD. This project seeks to elucidate the role of Prx6 in AD as well as the underlying mechanisms. *Drosophila* provide a convenient model for this investigation because they express two highly conserved homologs of mammalian Prx6: dPrx6005, with only peroxidase activity, and

dPrx2540, with both peroxidase activity and phospholipase-A_2 activity which may influence inflammation. If this phospholipase-A_2 activity promotes inflammation, dPrx2540 (and Prx6 in humans) could be exacerbating AD progression. Lifespan experiments show that flies under-expressing dPrx2540 in an AD background have significantly improved lifespan, suggesting that dPrx2540 may indeed exacerbate AD. Surprisingly, however, flies over-expressing dPrx2540 also had a small increase in lifespan, suggesting the role of dPrx2540 may be more complex. Further lifespan experiments, with greater expression levels of dPrx2540, are planned to tease apart the conundrum of beneficial results in both over- and under-expression experiments. Experiments measuring the expression of antimicrobial peptides as markers of inflammation suggest that neuronal expression of dPrx2540 alone or of $A\beta_{42}$ alone do not cause inflammation in fly heads. CRISPR methodology was used to generate flies with all endogenous copies of dPrx2540 removed (2540null) in order to more rigorously investigate the mechanisms of how dPrx2540 may influence AD. These 2540null flies exhibit reduced lifespan and fertility. Mutant dPrx2540 constructs with either peroxidase or phospholipase-A_2 activities ablated will be crossed into the dPrx2540null background and further into the AD background.

TABLE OF CONTENTS

LIST OF FIGURES

LIST OF TABLES

ACKNOWLEDGEMENTS

I would like to thank Dr. William Orr granting me the opportunity to study at SMU and for his invaluable guidance throughout this project. I also owe much to Nathan Drolet who taught me a great deal about lab work, especially during my first year. Dr. Vladimir Klichko and Dr. Svetlana Radyuk have provided critical advice and instruction. Thank you to my other committee members: Dr. Adam Norris and Dr. Pia Vogel. Judith Benes has been a cornerstone of this project, maintaining the fly lab, assisting in experiments, and as another source of indispensable advice. The assistance of the many undergraduates in the Orr lab has been vital to my success and the success of this project. With special thanks to Sarah, Anh, Bronson, and Samantha. Finally, I would like to thank my family and friends for their patience and support.

CHAPTER 1
INTRODUCTION

1.1 Background

Alzheimer's Disease (AD) is the sixth leading cause of death in the United States and is the most common cause of dementia among older adults. Current treatments focus on managing and, hopefully, retarding the symptoms of the disease. However, the successful treatment of the cellular and molecular processes underlying this disease is still out of reach. AD pathology is characterized by extra cellular plaques of the protein amyloid-β_{42} ($A\beta_{42}$), $A\beta_{42}$ oligomers, and neurofibrillary tangles of hyperphosphorylated Tau. Such pathology tends to start in the hippocampus and cortex, but slowly spreads throughout the brain as the disease progresses. The toxic protein aggregates impair the normal cellular processes of the affected neurons, leading to the characteristic neurodegeneration. Patients develop dementia and sometimes physical impairments. Death from Alzheimer's is often a result of complications induced by increasing systemic dysfunction [Alzheimer's Disease Fact Sheet, 2019].

In the current model, extra-cellular $A\beta_{42}$ plaques may actually serve a protective function while the $A\beta_{42}$ oligomers are thought to be a cause of toxicity [Castellani et al., 2009]. Tau, which normally binds to microtubules, mislocalizes when hyperphosphorylated, forming tangles and impeding cellular transport, especially in dendritic spines [Hoover et al., 2010]. These misfolded and mislocalized

proteins bind to pattern recognition receptors on glial cells, thus triggering an innate immune response including the release of inflammatory factors, including tumor necrosis factor-α (TNF-α) [Heneka et al., 2015]. Inflammation and protein aggregates lead to elevated oxidative stress (OS), including peroxidized lipids. In turn, such OS can promote further $A\beta_{42}$ deposition and hyperphosphorylation of Tau. It is likely that these factors play a key role in driving the neurodegeneration associated with Alzheimer's and similar diseases [Chen and Zhong, 2014].

Peroxiredoxins (Prx or Prdx) are ubiquitous regulators of reactive oxygen species (ROS), reducing peroxides and some reactive nitrogen species via thiol groups (-SH) of highly conserved catalytic cysteine residues, sometimes known as peroxidatic cysteines (C_P). As Prxs reduce peroxides, their C_P is oxidized, which contributes to regulating their structure and secondary functions. Therefore, Prxs can sense and react to changes in cellular redox state to drive various response pathways. Peroxiredoxins are subdivided into three general classes: (1) typical 2-Cys, (2) atypical 2-Cys, and (3) 1-Cys Prxs. All have a C_P, while 2-Cys Prxs also have a resolving cysteine (C_R) residue that is responsible for reducing the C_P, either in the same molecule (atypical), or in another Prx subunit (typical) [Ahn et al., 2018]. The C_P of a 1-Cys Prx is typically reduced by glutathione [Fisher, 2018].

Peroxiredoxin 6 (Prx6) is a 1-Cys Prx and localizes to both cytosol and lysosomes [Sorokina et al., 2009]. However, it is perhaps primarily important for its unique functions including, the ability to bind phospholipids, reduce phospholipid peroxides (PRX activity), intracellular phospholipase activity ($aiPLA_2$), and the transfer of fatty acyl CoA into the sn-2 position of lysophosphatidylcholine (LPCAT activity) [Fisher, 2018]. Importantly for AD, Prx6 is upregulated in the brains of patients, concentrated primarily in astrocytes, with smaller increases in expression in neurons [Power et al., 2008]. While over-expression of other

peroxiredoxins has been linked to improved stress resistance and lifespan, probably due primarily to their antioxidant functions, over-expression of Prx6 has been shown to exacerbate AD symptoms in mice [Radyuk and Orr, 2018] [Yun et al., 2013].

The PLA_2 activity of Prx6 hydrolyzes the sn-2 fatty acyl bond of phospholipids, releasing arachidonic acid, a precursor to pro-inflammatory eicosanoids, such as prostaglandins and leukotrienes [Dennis, 1994] [Saul et al., 2019]. The Prx6 PLA_2 active site consists of a catalytic triad of serine, histidine, and aspartate. Interestingly, secreted PLA_2 ($sPLA_2$) enzymes are important in the mammalian inflammatory response and have been found in venoms from several taxa, including insects, arachnids, and reptiles [Nicolas et al., 1997]. With both PRX and PLA_2 activities, Prx6 seems to have a role in regulating inflammation in response to oxidative damage to lipids. Although, PLA2 activity has been implicated in exacerbating neurodegenerative diseases, this has not been tested directly [Yun et al., 2013].

1.2 Hypothesis

At an axis point between OS and inflammation, Prx6 may have valuable therapeutic potential for treating AD. With the available information about Prx6 it may be that, in an AD background, the PLA_2 activity drives inflammation, resulting in increased deposition of protein aggregates, exacerbating the AD phenotype, which further increases OS, causing upregulation of Prx6 and thus, more PLA_2 activity.

Drosophila melanogaster, which are being used as a model organism in this study, possess two distinct homologs of Prx6, dPrx2540 and dPrx6005. dPrx2540 has the same

functions of human Prx6, while dPrx6005 lacks a PLA_2 catalytic site. Therefore, *Drosophila* are especially well equipped for testing the effects of Prx6 PLA_2 activity against an AD background. Given this, our hypothesis is that when dPrx2540 (with PRX and PLA_2 activity) is overexpressed in neurons of flies expressing human $A\beta_{42}$, the AD phenotype should be exacerbated, including reduced lifespan, reduced activity, impaired learning and memory, and increased neuronal inflammation. Under-expression of dPrx2540 in the AD fly model should somewhat alleviate the AD phenotype. Over-expression of dPrx6005 (PRX activity only), or dPrx2540 with PLA_2 activity ablated, in neurons of flies expressing human $A\beta_{42}$ should have a positive effect, due to PRX activity, compared to the AD background alone.

1.3 Objectives

The experiments performed for this project fall under two major objectives. The first objective is to determine whether dPrx2540 or dPrx6005 have an effect on the AD phenotype in *Drosophila*. This involves experiments to test survivorship, learning and memory, physical activity, and neuronal inflammation. The AD background phenotype was generated by tissue specific expression of a human $A\beta_{42}$ transgene in neurons. These experiments compare flies over-expressing or under-expressing, either dPrx2540 or dPrx6005, with and without the $A\beta_{42}$ background. My contribution to this objective included confirmation of dPrx6 transgene levels by immunoblot analysis, survivorship studies, and the assessment of inflammation via qPCR.

The second major objective is to determine whether the PRX or PLA_2 activity of dPrx2540 is responsible for any effect it has on the *Drosophila* AD model. To this end, CRISPR

methodology was used to delete all endogenous copies of dPrx2540, creating a "clean slate" *Drosophila* line with no Prx6 PLA_2 activity. Three dPrx2540 mutant lines were generated concurrently, one with an ablated PLA_2 active site, one with an ablated PRX active site, and a third in which both PLA_2 and PRX have been ablated. The plan from here is to cross the different mutant transgenes into the dPrx2540-null $A\beta_{42}$ background in order to directly test the hypothesis that PLA_2 activity exacerbates the AD phenotype.

CHAPTER 2
METHODS

2.1 The Gal4-UAS System and Experimental Crosses

The Gal4-UAS system was adapted from yeast and provides a powerful tool for controlling tissue specific expression of a transgene in *Drosophila*. Gal4 is a transcription factor that binds to UAS elements to induce transcription at the downstream start site. A Gal4 driver construct consists of a Gal4 gene under control of a tissue specific promoter. The target construct consists of a UAS-element upstream of the transgene we are interested in expressing [Chow, 2017]. The driver constructs used for this project were inserted into a *Drosophila* chromosome via P-element plasmids to make the "driver line". The target constructs were inserted in a similar manner into a separate "target line." Both driver and target lines have been generated from the same *yellow-white (yw) Drosophila* background line. The transgene of interest, such as dPrx2540 or human $A\beta_{42}$, will not be expressed until the driver line is crossed to the target line. The progeny of this experimental cross will express any UAS-element transgenes present in its genome. It is also important that the Gal4-UAS system is temperature sensitive, allowing another level of control over transgene expression. Higher temperatures cause an increase in Gal4 activity [Brand et al., 1994].

Driver and target lines were raised separately in standard agar food bottles with 5mL/L tetracycline added to minimize the risk of bacterial infection being transmitted to their progeny,

without directly influencing the health of the experimental flies. These flies were collected and females from the driver line were crossed with males from the target line. Control crosses (transgene x *yw* and driver x *yw*) corresponding to each experimental cross (transgene x driver) were also made to account for any effects from transgene insertion. The progeny generated from these crosses are the experimental flies, which are collected into fresh food vials with standard agar food. All experimental crosses and offspring were raised at 28ºC to enhance transgene expression. Specific drivers and transgenes will be detailed for each experiment.

2.2 Transgenic *Drosophila* Lines

Table 2.1 contains a list and descriptions of the fly lines used for this project. These fly lines were generated by P-element based insertion of UAS-transgenes. Lines Aβ33773 and Aβ33774 were purchased from the Bloomington Drosophila Stock Center. Line Aβ159 was generated at the Crowther lab at the University of Cambridge. Lines containing constructs for over- or under-expression of dPrx2540 or dPrx6005 were generated previously in this lab.

Abbreviation	Description
yw	Yellow-white mutant. This is the genetic background of the fly lines used for this project.
ELAV	Carries the Gal4 driver for neuronal expression. Located on the X chromosome.
Aβ33773	Carries the UAS-transgene for expression of human $A\beta_{42}$ (no driver). Located on the 2nd chromosome.
Aβ33774	Carries the UAS-transgene for expression of human $A\beta_{42}$ (no driver). Located on the 3rd chromosome.
Aβ159	Carries the UAS-transgene for expression of human $A\beta_{42}$ (no driver). Located on the 2nd chromosome (different insertion from Aβ33773).
dPrx6005	Carries the UAS-transgene for over-expression of dPrx6005 (no driver).
RNAi-dPrx6005	Carries the UAS-transgene for RNAi knockdown of dPrx6005 (no driver).
dPrx6005 + Aβ33773	A combination line carrying two UAS-transgenes. One for over-expression of dPrx6005 and another for expression of $A\beta_{42}$ (no driver).
RNAi-dPrx6005 + Aβ33774	A combination line carrying two UAS-transgenes. One for under-expression of dPrx6005 and another for expression of $A\beta_{42}$ (no driver).
dPrx2540	Carries the UAS-transgene for over-expression of dPrx2540 (no driver).
RNAi-dPrx2540	Carries the UAS-transgene for RNAi knockdown of dPrx2540 (no driver).
dPrx2540 + Aβ33773	A combination line carrying two UAS-transgenes. One for over-expression of dPrx2540 and another for expression of $A\beta_{42}$ (no driver).
RNAi- dPrx2540 + Aβ33774	A combination line carrying two UAS-transgenes. One for under-expression of dPrx2540 and another for expression of $A\beta_{42}$ (no driver).
Driver A > UAS-transgene X	Indicates flies with both the indicated driver and indicated transgene, thus driving expression of the transgene. For example, **ELAV > dPrx2540** flies are expressing the UAS-dPrx2540 transgene and should have higher levels of dPrx2540 protein than control flies.
2540null	Flies in which all three endogenous copies of dPrx2540 have been removed via CRISPR.

Table 2.1. Genotype abbreviations and descriptions of the Drosophila lines used for this project.

2.3 Protein Isolation and Western Blots

Expression of dPrx2540 and dPrx6005 was measured by immunoblot analysis. Flies were collected in 1.7mL micro-centrifuge tubes. Protein isolation was done with either 20-30 whole flies or 100-150 fly heads (whether whole flies or heads were used will be specified for individual experiments). Fly tissue was homogenized in lysis buffer (10μL/fly, with EDTA and protease inhibitors) by grinding with a powered pestle in the centrifuge collection tube. Homogenates were centrifuged for 5 minutes at 12,000g, 4°C. The supernatant was then transferred to a fresh centrifuge tube. An equal volume of 2X β-mercaptoethanol loading dye was added to the supernatant and the sample was boiled for 3 minutes. Protein concentrations were measured via Lowry assay on a UV-1800 Spectrophotometer (Shimadzu). The Lowry assay was performed using the Bio-Rad DC Protein Assay reagents and recommended protocol.

For the Western Blot assays, equal amounts of total protein for each sample were run through 13% polyacrylamide gels before being transferred to a nitrocellulose membrane. Next, the membranes were washed in a blocking solution of PBS-T and reconstituted milk. After blocking, the membranes were washed again in the same blocking solution with primary antibodies for either dPrx2540 or dPrx6005, as well as primary antibodies for actin. After treatment with primary antibodies, the membranes were washed in PBS-T, then washed again with blocking solution and horse radish peroxidase conjugated secondary antibodies. Excess antibodies were washed off with PBS-T and the membranes incubated with ECL Western Blot Prime Detection reagents (GeneSee Scientific) to generate the chemiluminescent reaction. The chemiluminescence was viewed and photographed with the Bio-Rad ChemiDoc Touch Imaging System. Protein band intensity was quantified with Bio-Rad Image Lab v5.2.1. Microsoft Excel was used to compare protein volumes given by the Bio-Rad software, normalizing to actin and

control samples. Primary antibodies used: mouse anti-actin C4 (1:2,500), rabbit anti-dPrx2540 (1:5,000), rabbit anti-dPrx6005 (1:2,500). Secondary antibodies used: HRP-conjugated anti-mouse (1:20,000) and HRP-conjugated anti-rabbit (1:20,000).

Before protein or RNA isolation procedures, fly heads were collected from experimental cohorts of 100-200 flies. Typically, 100 heads are enough for protein samples, but for RNA isolation, starting with 200 flies is useful for isolation of much more concentrated samples. The sample flies were collected and transferred to a 15mL graduated plastic tube which was then dipped in liquid nitrogen and shaken to separate heads, wings and legs, and thoraces/abdomens. After several successive freeze/shake cycles, the fly pieces are sifted through a three-part sieve. The top level (0.71mm) held thoraces/abdomens, the middle level (0.5mm) caught the heads, and the waste collection bowl at the bottom caught the wings and legs. The heads were transferred from the middle 0.5mm sieve to a 1.7mL microcentrifuge tube for later processing. The liquid nitrogen was also used to keep the flies, sieve, and sample tubes as cold as possible through this process to prevent condensation from causing fly heads to stick in the sieve and also to minimize sample degradation.

2.4 RNA Isolation and qPCR

RNA was isolated from fly heads using the TRIzol Reagent protocol (Ambion, Inc.), 200μL TRIzol/150 fly heads. RNA samples were assayed for concentration with a UV-1800 Spectrophotometer (Shimadzu). These samples were reverse transcribed (RT) using the ThermoFisher Maxima H Minus cDNA Synthesis Master Mix and its recommended protocol.

All RT samples in a given experiment started with a uniform amount of RNA, usually 4-6μg/30μL RT reaction, depending on the sample with lowest concentration. DNase treatment (optional with ThermoFisher's Master Mix) was done on the first set of samples. However, such DNase treatment was suspended because optimization tests revealed that, when performed carefully, the above protocols did not introduce significant DNA contamination and qPCR was more efficient without the optional treatment. Each qPCR run includes a negative RT control using Maxima H Minus no RT Master Mix (included with the kit from ThermoFisher) for each cDNA sample to ensure that there was no significant DNA contamination.

qPCR was performed with the GoTaq qPCR Master Mix (Promega) and primers specific to each AMP. Primers specific for RP49 were used to provide a positive reaction control from which to normalize total mRNA. For each cDNA-primer combination, experimental reactions were prepared as three 18μL technical replicates. qPCR reactions were run on a Rotor-Gene 3000 thermal cycler (Corbett Research). The cycling program heated the samples to 95ºC for 30 seconds, down to 50ºC for 30 seconds, and up to 72ºC for 30 seconds, repeated for 39 cycles.

2.5 DNA Isolation, PCR, and Electrophoresis

DNA was isolated from samples of 5-30 whole flies, depending on how many were available from a given cross or experiment. Protocols and materials were from either the Quick-DNA Universal kit (Zymo Research) or QuickDNA MiniPrep Plus kit (Zymo Research). DNA concentration was measure with a UV-1800 spectrophotometer (Shimadzu) to ensure an adequate concentration before proceeding to PCR.

Analytical PCR reaction mixes contained 5µL GoTaq Hot Start Master Mix (Promega), 0.5µL each of 10mM forward and reverse primers, 1-2µL of DNA template, and filled to 10µL total volume with nuclease-free water. A Mastercycler Personal (Eppendorf) thermal cycler was used for the PCR run with 31 cycles. Annealing temperatures were adjusted for optimal primer conditions and extensions times adjusted to account for expected product length.

Electrophoresis gels were made with 0.5X TAE buffer, 1.4% agarose, and ethidium bromide. The TAE buffer was diluted from a 10X stock made with 48.4g Tris base, 11.4mL glacial acetic acid, 3.7g of EDTA, then filled to 1L with MilliQ water. The RunOne Electrophoresis Cell (EmbiTec) was filled with 0.5X TAE buffer and about 1µL of extra ethidium bromide to ensure that DNA bands would be easily visible. A DNA molecular weight ladder was run beside samples to measure band sizes. Either ECON RCR DNA Ladder (Apex) or the 1kb DNA Ladder (GibcoBRL) were used for the ladder. The electrophoresis was generally run at 100 volts and a ChemiDoc Touch Imaging System (Bio-Rad) was used to acquire images of the results.

2.6 Lifespan Experiments

For all lifespan analyses, experimental flies were raised at 28^{o}C and collected into food vials (25 flies/vial) under CO_2-induced anesthesia. Each experimental condition and corresponding controls started with a total of 125 flies in 5 vials. Throughout the experiment the 28^{o}C temperature and 12h light/12h dark (08:00 to 20:00) cycle was maintained. Flies were transferred to fresh food vials every day. Each day during the vial transfer, the number of dead

flies was recorded, and the dead flies were removed. Mortality tracking data was entered into Prism 5.0c or Prism 8 (GraphPad Software, Inc.) to generate survivorship curves and statistical analysis.

2.7 Fertility Assay

The fertility assay was performed by pair mating age-matched virgin flies. *yw* males were mated to *yw* females and similarly, 2540null males mated to 2540null females. Each replicate consisted of one male and one female placed into a standard food vial. Twenty replicates of each condition were generated and kept at 25ºC with a 12h light/12h dark (08:00 to 20:00) cycle. Every day, each mated pair was transferred to a fresh food vial to help prevent overcrowding of offspring. As they began eclosing, the offspring of each mated pair were counted and removed from the vials. Data was analyzed and graphed with Prism 8 (GraphPad Software, Inc.).

2.8 CRISPR

The plasmid pCFD3 (Figure 2.1, top) was used to insert the gRNA for deletion of dPrx2540-1 and dPrx2540-3. dPrx2540-3 is located just downstream of dPrx2540-1, running in the opposite direction. The single gRNA (sequence: ATCAAACAGCAAGATGCGTTTGG) targets the first exon of dPrx2540-1 and the first exon of dPrx2540-3. The gRNA

oligonucleotide was ligated into pCFD3 between the dU6-3 promoter and the gRNA scaffold. The pCFD4 plasmid (Figure 2.1, bottom) was used to insert the two gRNAs targeting sequences upstream and downstream of dPrx2540-2 (upstream: AACGTGATCGACGTAAATAG) (downstream: GAATGGATCACAAATGGGGAA). The first gRNA oligonucleotide was ligated into pCFD4 between the dU6-1 promoter and the corresponding gRNA scaffold. The second gRNA oligonucleotide was ligated into pCFD4 between the dU6-3 promoter and corresponding gRNA scaffold. Plasmids were sent to Retrogen, Inc. for sequencing to confirm insertion of the gRNAs, then sent to BestGene, Inc. for injection into *Drosophila* embryos. Flies expressing the gRNAs were crossed with flies expressing a Cas9 transgene under the control of the *nanos* promoter for germline specific expression.

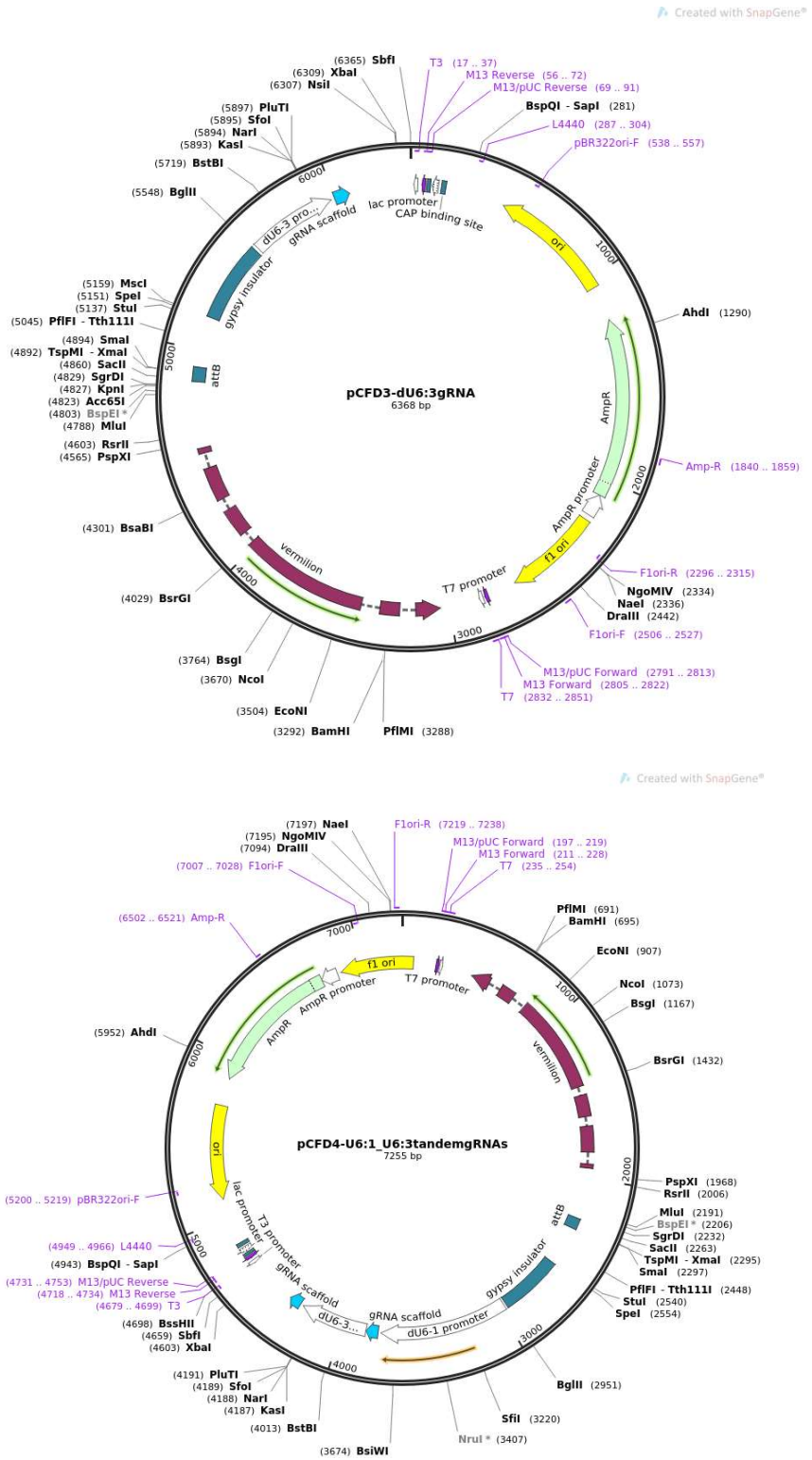

Figure 2.1. Maps of the pCFD3 and pCFD4 plasmids used to insert gRNA transgenes. [Addgene, 2019]

2.9 Molecular Cloning

The DNA fragment to be used for cloning, such as dPrx2540, was amplified via PCR using the Q5 High-Fidelity 2X Master Mix (New England Biolabs). The amplified fragment was isolated from a sterilized agarose gel and purified using the QIAquick Gel Extraction Kit (Qiagen). Restriction digestion of the pUAST plasmid (Figure 2.2) was done with FastDigest BglII and FastDigest XhoI in 10X FastDigest Buffer (ThermoFisher) using the recommended protocol from ThermoFisher. The desired plasmid fragments were then extracted from agarose gels as mentioned above. Ligation of DNA fragment into the plasmid was done with T4 DNA Ligase, 10X T4 DNA Ligase Buffer, and T4 polynucleotide kinase from New England Biolabs using their recommended protocol [New England Biolabs, 2019]. Plasmids were then transformed into DH5α *E. coli* via heat shock at 42ºC for 30 seconds to encourage plasmid uptake. Afterwards, the *E. coli* were incubated in SOC media and plated onto ampicillin (100mg/mL) LB agar. Transformed colonies were selected for ampicillin resistance, then re-streaked on ampicillin LB agar. Clonal colonies were tested by PCR for the presence of the plasmid containing the desired transgene construct. Large scale cultures for plasmid preparations were grown in LB liquid media. Plasmids were sent to GeneWiz for sequencing to confirm the presence of the transgene construct, then sent to Best Gene, Inc. for injection into *Drosophila* embryos.

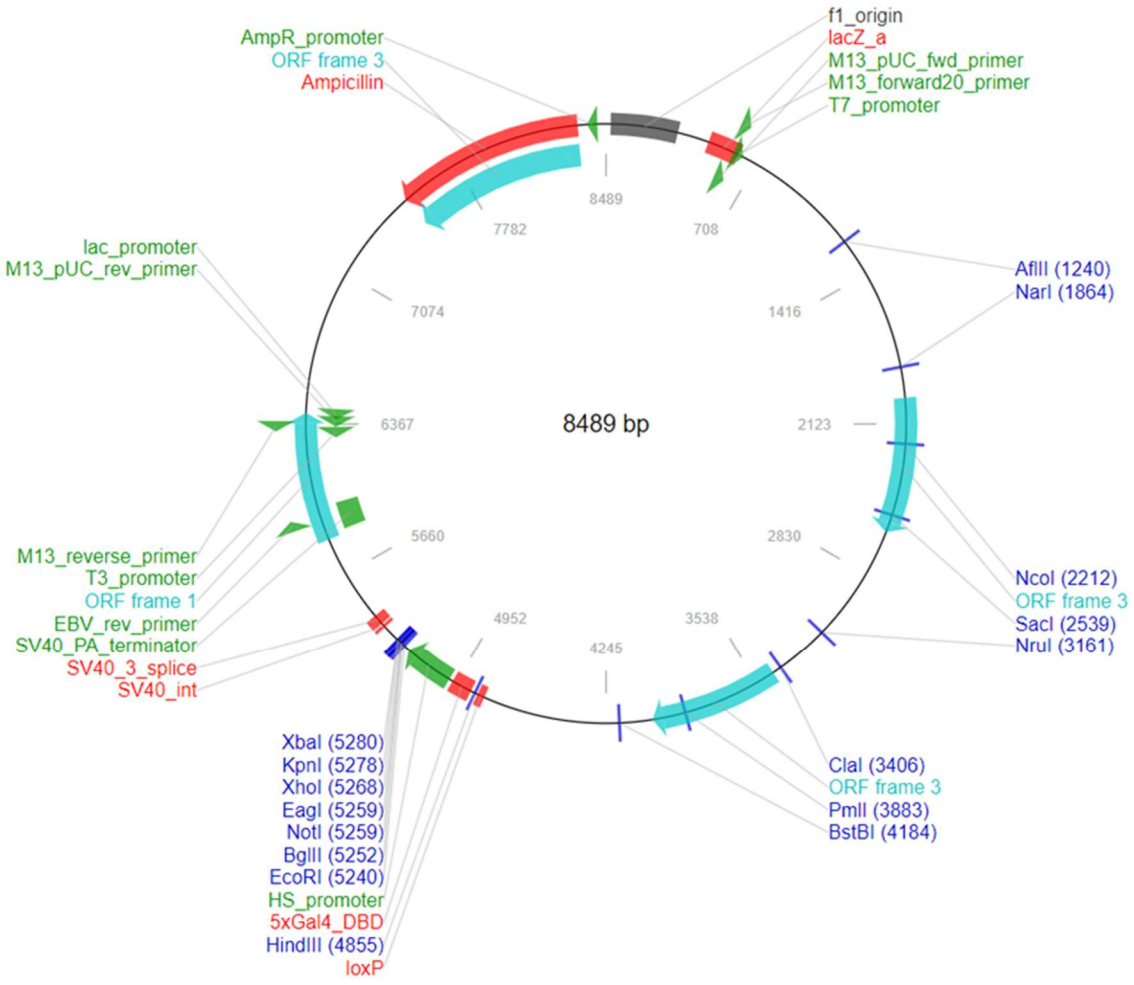

Figure 2.2. Map of the pUASTattB plasmid used as the insertion vector for UAS-dPrx2540, UAS-dPrx6005, and UAS-dPrx2540 mutant transgenes. cDNA for the desired gene was ligated into the plasmid between the BglII and XhoI restriction sites. [Addgene, 2019]

CHAPTER 3
RESULTS

3.1 CRISPR Deletion of Endogenous dPrx2540

Drosophila have three copies of dPrx2540 (dPrx2540-1, -2, -3) clustered together on chromosome 2. However, there are two putative genes located between dPrx2540-2 and dPrx2540-1/3, so all three copies could not be removed at once [Thurmond et al. 2019]. Instead, the deletion was done in two stages. First, dPrx2540-2 was deleted by crossing flies expressing *nos*-Cas9 (germline expression) with flies expressing gRNAs flanking dPrx2540-2 (Figure 3.1).

Germline expression of Cas9 causes the target locus to be deleted only in the germline of the F1 generation, then the F2 generation carries the deletion in all cells. Pair mating was used to cross the F1 generation with *glazed/CyO* mutant flies for screening and tracking of the deletion. 300 pair matings were done for the deletion of dPrx2540-2 due to the expectation of low efficiency. 5 of these 300 pair matings produced offspring carrying the deletion (hereafter Δ2540-2). Second, *nos*-Cas9 expressing flies were crossed with flies expressing gRNAs (in the Δ2540-2 background) flanking both dPrx2540-1 and dPrx2540-3 (Figure 3.1).

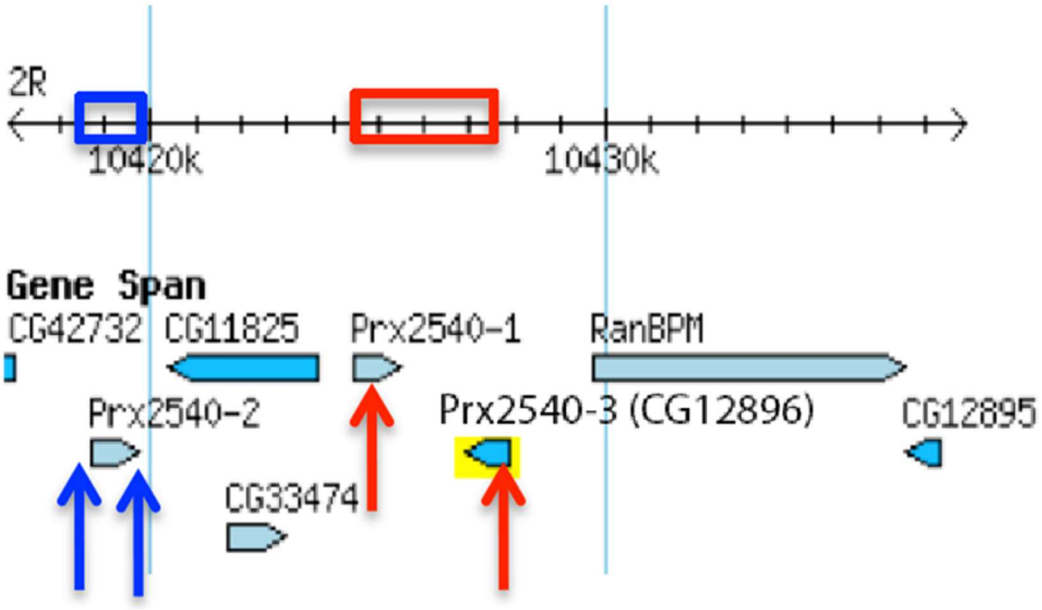

Figure 3.1. FlyBase map of the region of *Drosophila* chromosome 2 containing the three copies of dPrx2540 [Thurmond et al. 2019]. The blue box and blue arrows indicate gRNA target sites for deletion of dPrx2540-2. The red box and red arrows indicate gRNA target sites for deletion of dPrx2540-1/3.

For the second deletion, a total of 600 pair matings produced two lines carrying the Δ2540-1/-3 deletion. The deletions were screened with PCR (Figure 3.2) and confirmed by sequencing performed by GeneWiz (not shown). The deletion of all 3 copies of dPrx2540 (hereafter 2540null) was further confirmed by western blot to ensure no endogenous production of dPrx2540 protein (Figure 3.3).

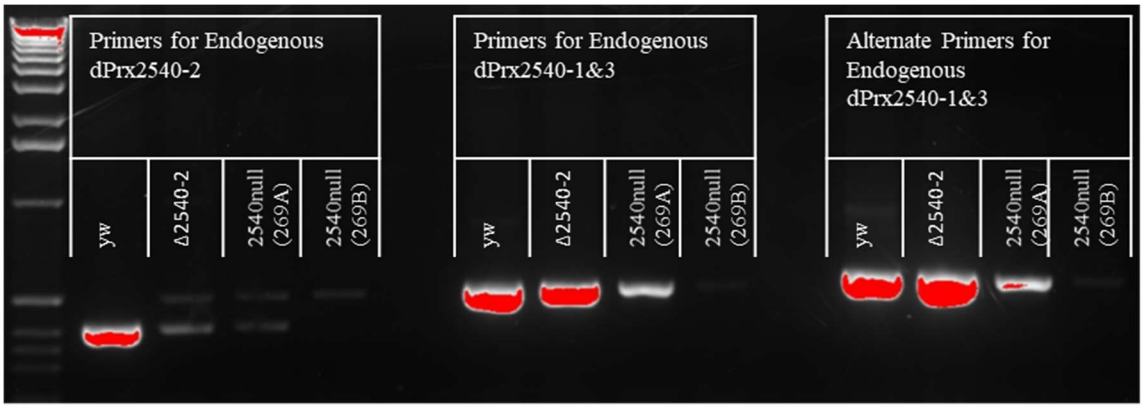

Figure 3.2. PCR confirmation of deletion of all three copies of dPrx2540. No amplification is seen from any of the three primer sets for the 2540null-269B cohort. A relatively strong band appears with both sets of dPrx2540-1/3 primers in the 269A cohort, indicating contamination in the population. The deletions in 269B were further confirmed by sequencing (not shown).

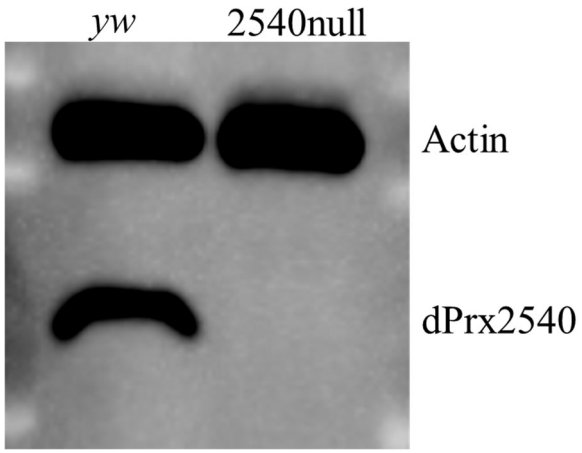

Figure 3.3. Western blot confirmation of the deletion of all endogenous dPrx2540 genes. The image shows dPrx2540 expression in *yw* (genetic background) and 2540null flies.

To characterize the 2540null phenotype, lifespan and fertility assays are being performed, comparing 2540null flies to the *yw* background from which they were generated. Though, still in progress, the fertility assay reveals a significant reduction in offspring produced by 2540null flies compared to the *yw* background (Figure 3.4). Ongoing survivorship experiments show a significant reduction in the lifespan of 2540null flies compared to *yw* for both males and females (Figure 3.5). It is somewhat expected that 2540null flies would have impaired health given the reported function for Prx6 in peroxidized membrane repair [Fisher, 2017]. Lipid peroxidation and activity assays are also planned to further characterize the 2540null flies.

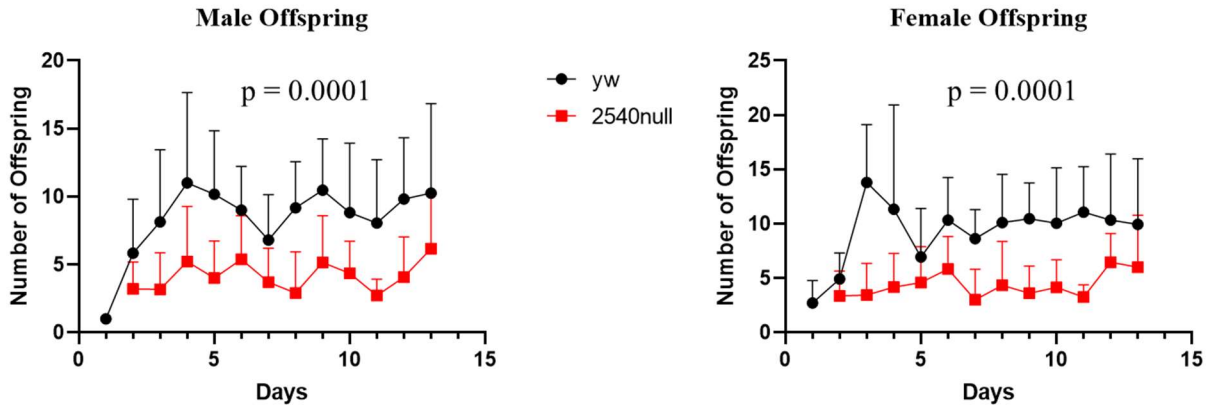

Figure 3.4. Fertility assay comparing 2540null and *yw* flies. Each point indicates the average offspring produced on a particular day across all replicates. Error bars indicate standard deviation between replicates. Black = *yw* control. Red = 2540null. *P* values were calculated with the unpaired two-tailed t test.

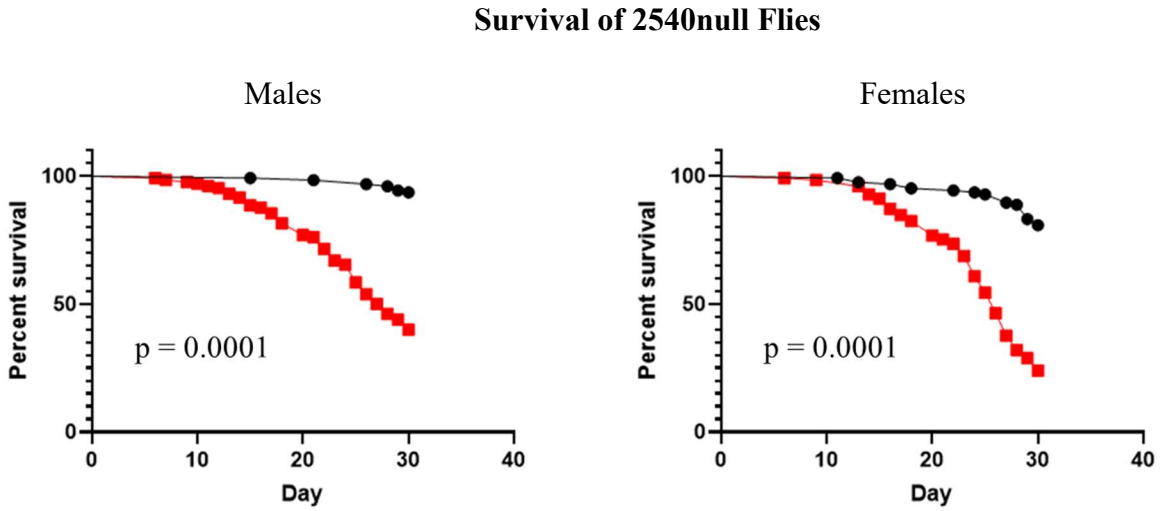

Figure 3.5. Survivorship graphs of 2540null flies compared to the *yw* background. Red = 2540null. Black= *yw*. *P* values were calculated using the log-rank (Mantel-Cox) test.

Interestingly, *Drosophila* may have a compensatory mechanism for expression of dPrx6. Between the three copies of dprx2540, dPrx2540-2 has the highest reported expression [Thurmond et al., 2019]. Yet, flies with dPrx2540-2 deleted from their genome, showed no significant difference in expression of dPrx2540 protein compared to *yw* flies (Figure 3.6).

Expression of dPrx2540 in Flies with Deletion of dPrx2540-2

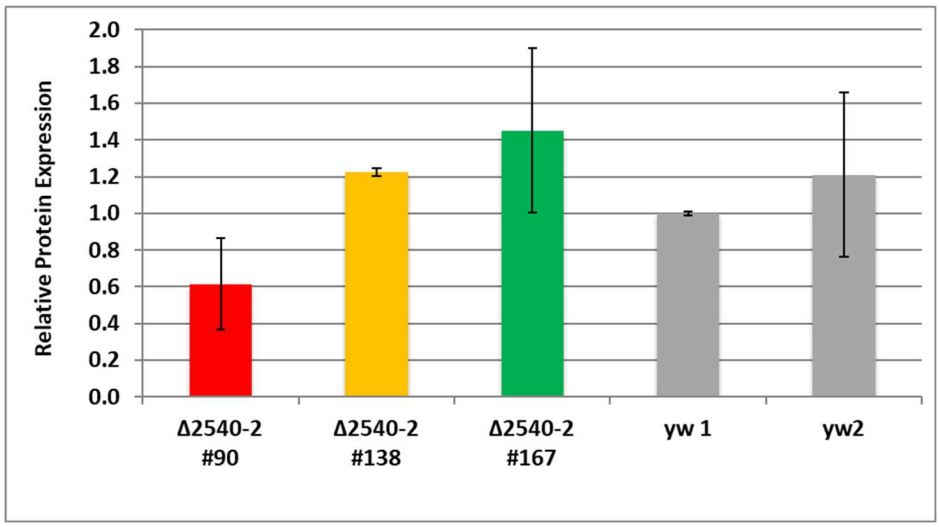

Figure 3.6. Possible compensation of dPrx2540 protein expression in Δ2540-2 flies. The graph shows the quantification of two western blots testing expression of dPrx2540 in three Drosophila lines in which dPrx2540-2 was successfully removed via CRISPR. There is no significant and consistent change in dPrx2540 expression due to the deletion. Error bars indicate standard deviation between two experiments.

3.2 Lifespan Analysis of Flies Expressing dPrx6 in an AD Background

As discussed in Chapter 1.3, AD causes several symptoms in humans that can be measured in a *Drosophila* model of AD. Flies expressing transgenic constructs of human "arctic" $A\beta_{42}$ experience neurodegeneration and early death, reducing their average lifespan by half or more [Crowther et al., 2005]. If PLA_2 activity exacerbates AD symptoms as expected, overexpressing dPrx2540 (with PLA_2 activity) in flies also expressing $A\beta_{42}$ (the AD background) should result in a further decrease in lifespan. Conversely, under-expressing dPrx2540 in the AD background flies should have an opposite effect, extending their lifespan. Over-expression of dPrx6005 (without PLA_2 activity) should have little effect on the AD background or possibly even a beneficial effect from the PRX activity reducing OS.

For the lifespan experiments, combination AD + dPrx2540 lines with the highest (over-expressor) or lowest (under-expressor) dPrx2540 expression were selected for the experimental crosses. Transgenic line UAS-Aβ33773, over.2540 B1 (hereafter shown as dPrx2540 + Aβ33773) was chosen for over-expression in the AD background and line UAS-Aβ33774, RNAi-2540-8ds A1 (hereafter shown as RNAi-dPrx2540 + Aβ33774) was chosen for under-expression in the AD background. ELAV-Gal4 (hereafter shown as ELAV) was chosen as the driver because it drives transgene expression specifically in neurons. Transgenic lines were crossed to ELAV lines to generate experimental flies (ELAV > dPrx2540 + Aβ33773 or ELAV > RNAi-dPrx2540 + Aβ33774) or crossed to *yw* to generate control lines. Transgenic lines expressing only Aβ33773 or Aβ33774 (ELAV > Aβ33773 or ELAV > Aβ33774), were also generated to create the AD background for comparison. Two separate lifespan experiments have been performed to examine the effect of dPrx2540 expression against an AD background. In the same manner, a single experiment has been conducted to test the effect of dPrx6005 expression

against an AD background. The relative expression of dPrx6005 in experimental and control lines is shown in Figure 3.7. and relative expression of dPrx2540 is shown in Figure 3.8.

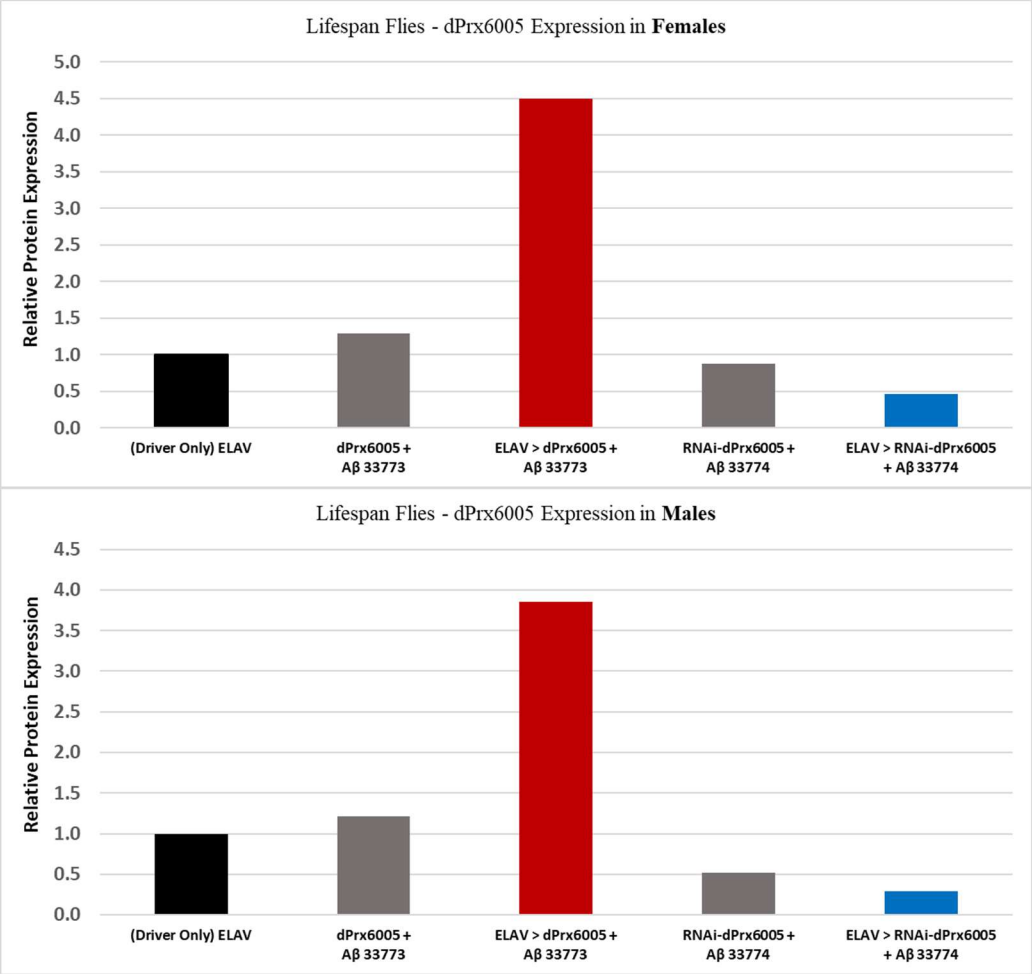

Figure 3.7. Western blot quantification of dPrx6005 expression in fly heads. These fly lines were used for the lifespan assay to determine the effect of dPrx6005 expression on the AD background. Expression is shown relative to ELAV (driver only) and normalized to actin. Grey bars = control lines. Black bar = ELAV control. Red bars = dPrx6005 over-expression lines. Blue bars = dPrx6005 under-expression lines.

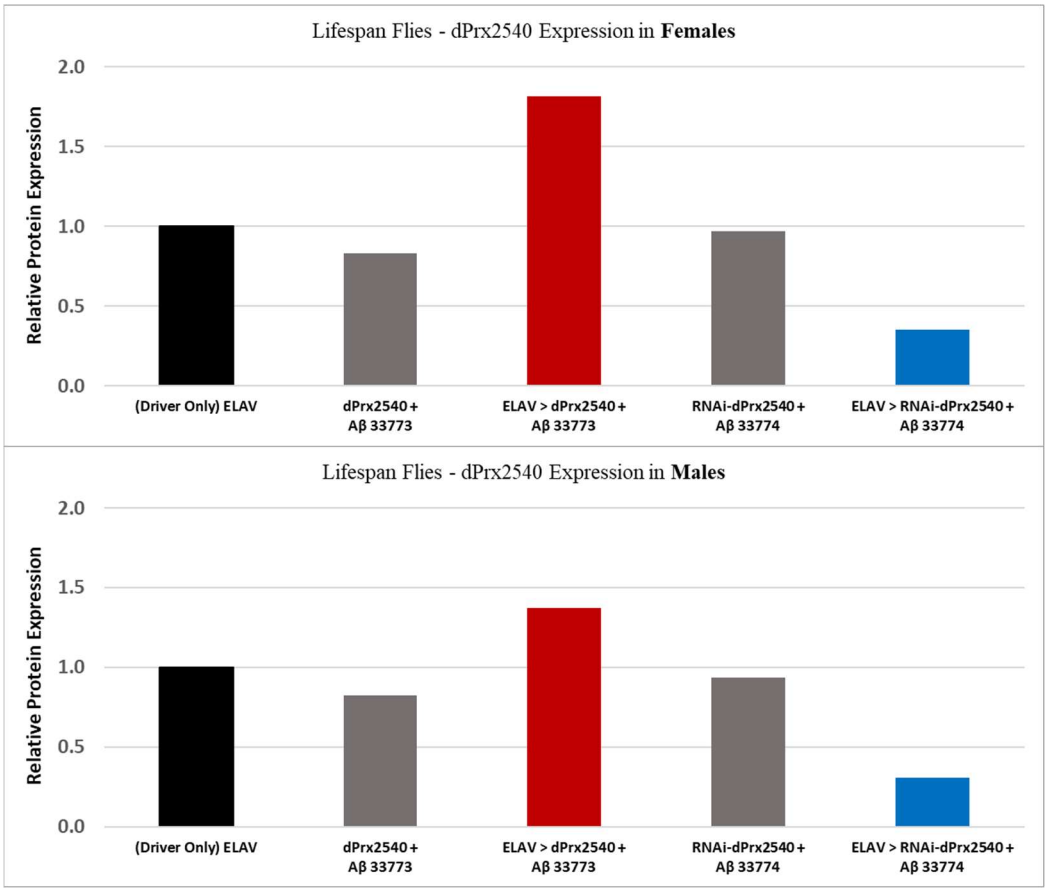

Figure 3.8. Western blot quantification of dPrx2540 expression in fly heads. These fly lines were used for the lifespan assay to determine the effect of dPrx2540 expression on the AD background. Expression is shown relative to ELAV (driver only) and normalized to actin. Grey bars = control lines. Black bar = ELAV control. Red bars = dPrx2540 over-expression lines. Blue bars = dPrx2540 under-expression lines.

Male flies overexpressing dprx6005 in the AD background (ELAV > dPrx6005 + Aβ33773) showed no significant change in lifespan compared to the AD background alone (ELAV > Aβ33773). Somewhat unexpectedly, males under-expressing dPrx6005 in the AD background (ELAV > RNAi-dPrx6005 + Aβ33774) showed a significant increase in lifespan compared to the AD background alone (ELAV > Aβ33774) (Figure 3.9, top panels and Table 3.1). Female flies overexpressing dPrx6005 in the AD background show a significant increase in lifespan compared to the AD background (Figure 3.9, bottom panels and Table 3.1). Female flies under-expressing dPrx6005 in the AD background also showed a significant increase in lifespan compared to the AD background. Interestingly, the increase in lifespan due to under-expression of dPrx6005 appears to be larger than that resulting from over-expression of dPrx6005, though both comparisons to the AD background share the same p-value (Figure 3.9, bottom panels and Table 3.1). ELAV > dPrx6005 median lifespan was similar to the *yw* genetic background and greater than ELAV alone, thus over-expression of dPrx6005 alone seems to have little to no effect on fly lifespan (data not shown). ELAV > RNAi-dPrx6005 median lifespan was greater than all other experimental and control lines for males and females (data not shown). Suppressing expression of dPrx6005 had a beneficial effect with and without $A\beta_{42}$ expression. PRX activity in some other peroxiredoxins is known to be beneficial, extending lifespan and enhancing oxidative stress resistance [Radyuk and Orr, 2018], so it is puzzling that a reduction in dPrx6005, with PRX activity only, would have a beneficial effect.

Survival of Flies Expressing dPrx6005 in an AD Background

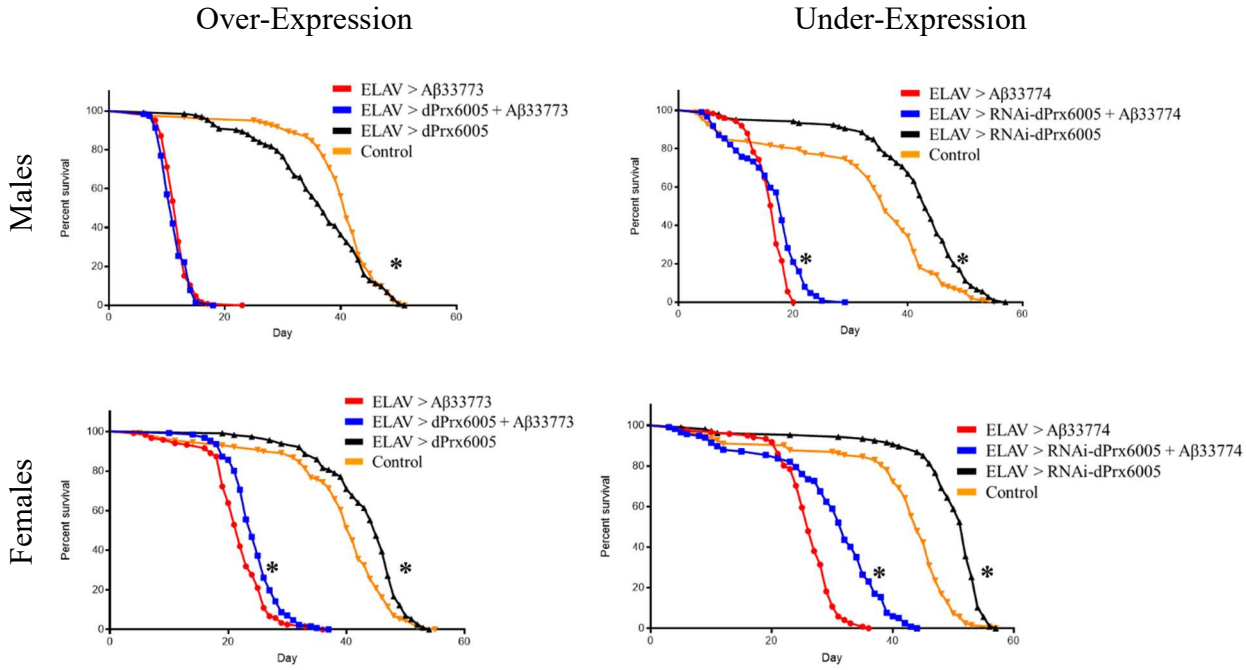

Figure 3.9. Survivorship graphs of flies comparing the effects of dPrx6005 expression in the AD background. Top panels show data from males. Bottom panels show data from females. After experimental crosses, all flies had a single copy of the ELAV driver and a single copy of each UAS-transgene. Asterisks indicate significant differences (see Table 3.1).

In the first lifespan experiment to analyze the effects of dPrx2540 expression (Figure 3.10, top panels and Table 3.2), male flies overexpressing dPrx2540 in the AD background (ELAV > dPrx2540 + Aβ33773) did not display a significant change in lifespan compared to flies expressing $A\beta_{42}$ alone (ELAV > Aβ33773). This seems to be contrary to the working hypothesis that dPrx2540 should exacerbate the AD phenotype. However, males under-expressing dPrx2540 in the AD background (ELAV > RNAi-dPrx2540 + Aβ33774) showed an increase in median lifespan as well as a large increase in maximum lifespan compared to flies expressing $A\beta_{42}$ alone (ELAV > Aβ33774). Males under-expressing dPrx2540 alone, without Aβ33774 (ELAV > RNAi-dPrx2540), had a reduced median lifespan compared to the control.

Survival of Flies Over-Expressing dPrx6005 in an AD Background

Males

Genotype	Median Lifespan	P Value (effect)	Compared to
ELAV > Aβ33773	12		
ELAV > dPrx6005 + Aβ33773	11	0.2 (ND)	ELAV > Aβ33773
Control	41		
ELAV > dPrx6005	37	0.0371 (decrease)	Control

Females

Genotype	Median Lifespan	P Value (effect)	Compared to
ELAV > Aβ33773	22		
ELAV > dPrx6005 + Aβ33773	24	0.0001 (increase)	ELAV > Aβ33773
Control	41		
ELAV > dPrx6005	45	0.0003 (increase)	Control

Survival of Flies Under-Expressing dPrx6005 in an AD Background

Males

Genotype	Median Lifespan	P Value (effect)	Compared to
ELAV > Aβ33774	17		
ELAV > RNAi-dPrx6005 + Aβ33774	18	0.0001 (increase)	ELAV > Aβ33774
Control	36		
ELAV > RNAi-dPrx6005	43	0.0001 (increase)	Control

Females

Genotype	Median Lifespan	P Value (effect)	Compared to
ELAV > Aβ33774	26		
ELAV > RNAi-dPrx6005 + Aβ33774	32	0.0001 (increase)	ELAV > Aβ33774
Control	44		
ELAV > RNAi-dPrx6005	52	0.0001 (increase)	Control

Table 3.1. Comparison of survivorship curves for flies expressing dPrx6005 in an AD background. *P* values were calculated using the log-rank (Mantel-Cox) test. Effects listed in parentheses are interpretations based on median lifespans and visual analysis of the survivorship curves.

The second experiment with dPrx2540 yielded slightly different results (Figure 3.10, bottom panels and Table 3.2). Males overexpressing dPrx2540 in the AD background showed a significant increase in median lifespan compared to the AD background line, which was not consistent with the first experiment. As in the first experiment, ELAV > RNAi-dPrx2540 + Aβ33774 produced a beneficial effect on median lifespan compared to ELAV > Aβ33774. Again, knocking down dPrx2540 in the absence of Aβ33774 actually reduced median lifespan compared to the control, which may be important given the nascent results in the lifespan assay with the 2540null flies (Figure 3.5). There seemed to be a trend towards an increase in maximum lifespan in males under-expressing dPrx2540 in the AD background compared to the AD background alone, though this was reversed in the last surviving 10% due to a few strangely long-lived flies despite expression of $A\beta_{42}$. It is notable that under-expression of dPrx2540 or dPrx6005 produced a larger increase in lifespan in males.

Interestingly, despite strong positive effects on lifespan from over- and under-expression of dPr6005, female flies showed much weaker effects from over- and under-expression of dPrx2540 in the AD background compared to the results with male flies (Figure 3.11 and Table 3.3). In the first experiment analyzing the effects of dPrx2540 expression, female flies of ELAV > dPrx2540 + Aβ33773 showed no change in lifespan compared to the ELAV > Aβ33773. Female flies of ELAV > RNAi-dPrx2540 + Aβ33774 had a large increase in median lifespan and maximum lifespan when compared to ELAV > Aβ33774. For female flies, the repeat of this experiment gave less consistent results than those seen with males. ELAV > dPrx2540 + Aβ33773 showed a mild, but significant, increase in median lifespan, while ELAV > RNAi-dPrx2540 + Aβ33774 showed no change compared to the AD background alone.

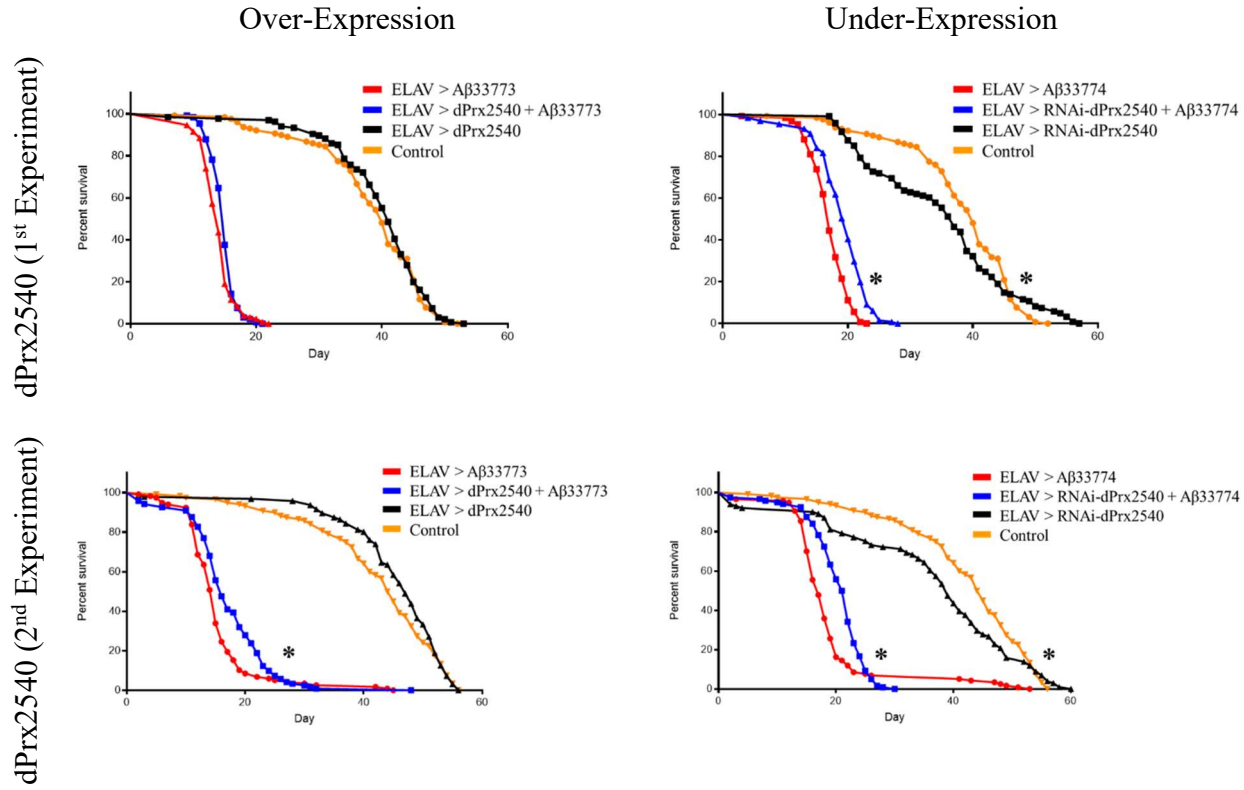

Figure 3.10. Survivorship graphs of male flies comparing the effects of dPrx2540 expression in the AD background. Data from two separate experiments are shown: (top) the 1st lifespan experiment testing the effects of dPrx2540 expression, and (bottom) repeat of the lifespan experiment testing the effects of dPrx2540 expression. After experimental crosses, all flies had a single copy of the ELAV driver and a single copy of each UAS-transgene. Asterisks indicate significant differences (see Table 3.2).

Survival of Male Flies Over-Expressing dPrx2540 in an AD Background

1st Experiment

Genotype	Median Lifespan	P Value (effect)	Compared to
ELAV > Aβ33773	14		
ELAV > dPrx2540 + Aβ33773	15	0.0091 (ND)	ELAV > Aβ33773
Control	40		
ELAV > dPrx2540	41	0.4106 (ND)	Control

2nd Experiment

Genotype	Median Lifespan	P Value (effect)	Compared to
ELAV > Aβ33773	15		
ELAV > dPrx2540 + Aβ33773	16	0.0019 (increase)	ELAV > Aβ33773
Control	44.5		
ELAV > dPrx2540	47	0.2138 (ND)	Control

Survival of Male Flies Under-Expressing dPrx2540 in an AD Background

1st Experiment

Genotype	Median Lifespan	P Value (effect)	Compared to
ELAV > Aβ33774	17		
ELAV > RNAi-dPrx2540 + Aβ33774	20	0.0001 (increase)	ELAV > Aβ33774
Control	40		
ELAV > RNAi-dPrx2540	37	0.3895 (decrease)	Control

2nd Experiment

Genotype	Median Lifespan	P Value (effect)	Compared to
ELAV > Aβ33774	17		
ELAV > RNAi-dPrx2540 + Aβ33774	21.5	0.0001 (increase)	ELAV > Aβ33774
Control	44.5		
ELAV > RNAi-dPrx2540	39	0.1111 (decrease)	Control

Table 3.2. Comparison of survivorship curves for male flies expressing dPrx2540 in an AD background. *P* values were calculated using the log-rank (Mantel-Cox) test. Effects listed in parentheses are interpretations based on median lifespans and visual analysis of the survivorship curves.

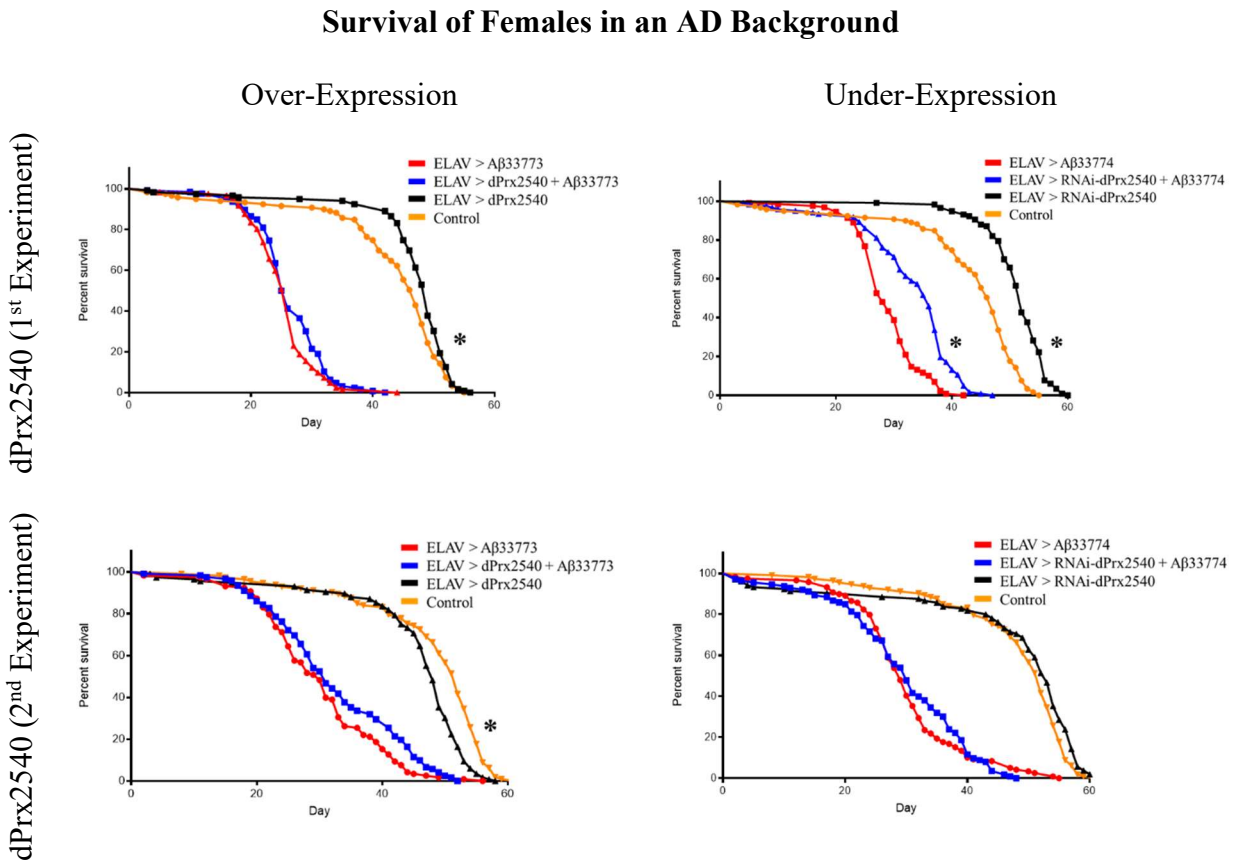

Figure 3.11. Survivorship graphs of female flies comparing the effects of dPrx2540 expression in the AD background. Data from two separate experiments are shown: (top) the 1st lifespan experiment testing the effects of dPrx2540 expression, and (bottom) repeat of the lifespan experiment testing the effects of dPrx2540 expression. After experimental crosses, all flies had a single copy of the ELAV driver and a single copy of each UAS-transgene. Asterisks indicate significant differences (see Table 3.3).

Survival of Female Flies Over-Expressing dPrx2540 in an AD Background

1st Experiment

Genotype	Median Lifespan	P Value (effect)	Compared to
ELAV > Aβ33773	27		
ELAV > dPrx2540 + Aβ33773	25.5	0.1873 (ND)	ELAV > Aβ33773
Control	47		
ELAV > dPrx2540	49	0.005 (increase)	Control

2nd Experiment

Genotype	Median Lifespan	P Value (effect)	Compared to
ELAV > Aβ33773	33		
ELAV > dPrx2540 + Aβ33773	31	0.0367 (ND)	ELAV > Aβ33773
Control	52		
ELAV > dPrx2540	48	0.0001 (decrease)	Control

Survival of Female Flies Under-Expressing dPrx2540 in an AD Background

1st Experiment

Genotype	Median Lifespan	P Value (effect)	Compared to
ELAV > Aβ33774	28		
ELAV > RNAi-dPrx2540 + Aβ33774	36	0.0001 (increase)	ELAV > Aβ33774
Control	47		
ELAV > RNAi-dPrx2540	52	0.0001 (increase)	Control

2nd Experiment

Genotype	Median Lifespan	P Value (effect)	Compared to
ELAV > Aβ33774	29		
ELAV > RNAi-dPrx2540 + Aβ33774	30	0.9403 (ND)	ELAV > Aβ33774
Control	52		
ELAV > RNAi-dPrx2540	53	0.0298 (ND)	Control

Table 3.3. Comparison of survivorship curves for female flies expressing dPrx2540 in an AD background. *P* values were calculated using the log-rank (Mantel-Cox) test. Effects listed in parentheses are interpretations based on median lifespans and visual analysis of the survivorship curves.

The increase in lifespan due to over-expression of dPrx2540 could be explained by beneficial effects from the PRX activity, while the increase in lifespan due to under-expression of dPrx2540 could be explained by reduced PLA_2 activity as predicted by the hypothesis. Considering the relatively weak over-expression of dPrx2540 seen in the western blots (Figure 3.8), we reasoned that in order to observe the potential negative effects of PLA_2, stronger over-expression of dPrx2540 would need to be induced. To this end, flies with two copies of the ELAV driver, two copies of the dPrx2540 over-expression construct, and one copy of Aβ33773 were generated. Generation of flies with two copies of Aβ33773 was attempted, but this combination proved to be lethal. Two copies of the ELAV driver and two copies of Aβ33773 without dPrx2540 was also lethal. One copy of the AB33773 transgene should be enough because it is well established that this causes drastically shortened lifespan when expressed. A lifespan experiment with large over-expression of dPrx2540 using these double driver/double transgene flies is planned and should help clarify the effects of dPrx2540 in an AD background.

3.3 Neuroinflammation in Flies Expressing Aβ or dPrx2540

In *Drosophila*, the innate immune response is primarily controlled by the NF-κB pathways, Toll and IMD [Govind, 2008]. Part of this inflammatory response involves antimicrobial peptides (AMPs), small peptides that kill invading bacteria and fungi. Expression of these AMPs are induced through the Toll and IMD pathways. The Toll pathway responds to infection by Gram positive bacteria and fungi by producing Drosomycin, Attacins, Cecropins, and Defensins. The IMD pathway responds to infection by Gram negative bacteria by producing Diptericin, Attacins, and Cecropins [Imler and Bulet, 2005]. Expression of another innate defense factor, Turandot, is mediated by the JAK/STAT pathway in response to various stresses, such as infection, OS, and protein aggregates. Critically, pattern recognition receptors (PRRs), including Toll-like receptors (TLRs), also respond to endogenous damage associated molecular patterns (DAMPs) such as the misfolded and mislocalized $A\beta_{42}$ and Tau proteins that hallmark AD pathology [Morales et al., 2014]. Additionally, AD pathology has been reported to induce expression of TNF-α, a pro-inflammatory target of the NF-κB pathway, is also involved in activating apoptosis of damaged or infected cells [Heneka et al., 2015] [Wu and Zhou, 2010]. The Drosophila homolog of TNF-α is known as Eiger.

The hypothesis states that dPrx2540 exacerbates AD by promoting neuroinflammation through its PLA_2 activity. To test this, expression levels of the Attacin C, Cecropin, Defensin, Diptericin, Drosomycin, Eiger, and Turandot were measured in fly heads, via qPCR, as markers of neuroinflammation. These genes are expressed at very low levels in healthy cells, but expression increases dramatically with infection, loss of proteostasis, or age [Odnokoz et al., 2017]. Experimental flies were prepared as described in Chapter 2.1 and aged for 10 or 15 days. Flies of 15 days old or younger were used so that age-related inflammation did not produce false

positive results. Each day, the experimental flies were transferred to fresh food vials to reduce the risk of infection due to bacterial growth.

To test whether dPrx2540 expression alone could induce a neuroinflammatory response, the expression of five AMPs, Eiger, and Turandot was examined via qPCR in the heads of 10-day old flies with two copies (2x) of both the ELAV driver and the dPrx2540 transgene (2x ELAV > dPrx2540). In these lines ELAV drives neuronal expression of dPrx2540 to very high levels relative to controls (Figure 3.12). As shown in Figures 3.13 (Males) and 3.14 (Females), the experimental lines with 2x ELAV > dPrx2540 (2) and (3) do not show the large increase in expression of inflammatory markers, compared to controls, that would indicate a positive result. This experiment was also done with 2x ELAV > dPrx2540 lines (4) and (15) and with APPL driven dPrx2540 expression. APPL is the *Drosophila* ortholog of human APP, precursor to Aβ [Prüßing et al., 2013]. These additional experiments produced similar results (data not shown). Therefore, dPrx2540 over-expression alone, in neurons, does not appear to cause inflammation.

The particular *Drosophila* AD model used for these experiments, directly expressing human $A\beta_{42}$ from a UAS transgene, has been shown to cause early mortality in the experimental fly lines (see Chapter 3.2). However, inflammation due to $A\beta_{42}$ expression has not been confirmed in this AD model. Therefore, AMP expression was also tested in 10 and 15-day old fly heads of the $A\beta_{42}$ expressing *Drosophila* lines being used throughout this project. Typically, male flies expressing $A\beta_{42}$ begin dying in large numbers at ~10-15 days old, while controls tend to last 45 days or more at 28°C.

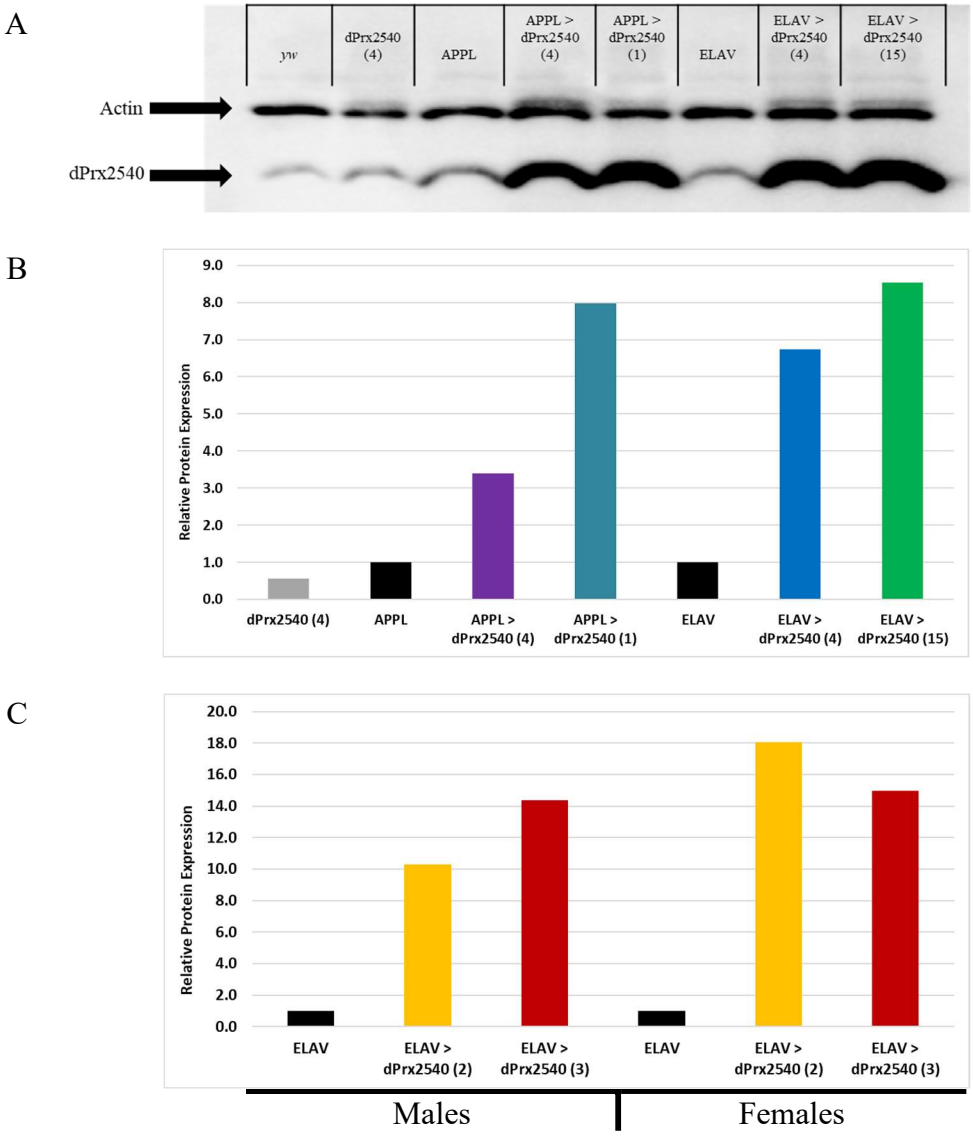

Figure 3.12. dPrx2540 Expression in 2x ELAV > dPrx2540 Flies. **(A)** Sample western blot showing dPrx2540 protein. **(B)** Quantification for the western blot shown in (A). **(C)** Quantification of dPrx2540 over-expression in lines (2) and (3). AMP expression for these flies is shown in figures 3.13 and 3.14. These experiments were conducted with 10-day old flies raised at 28ºC. Expression was calculated relative to the corresponding driver control (ELAV or APPL) and normalized to actin.

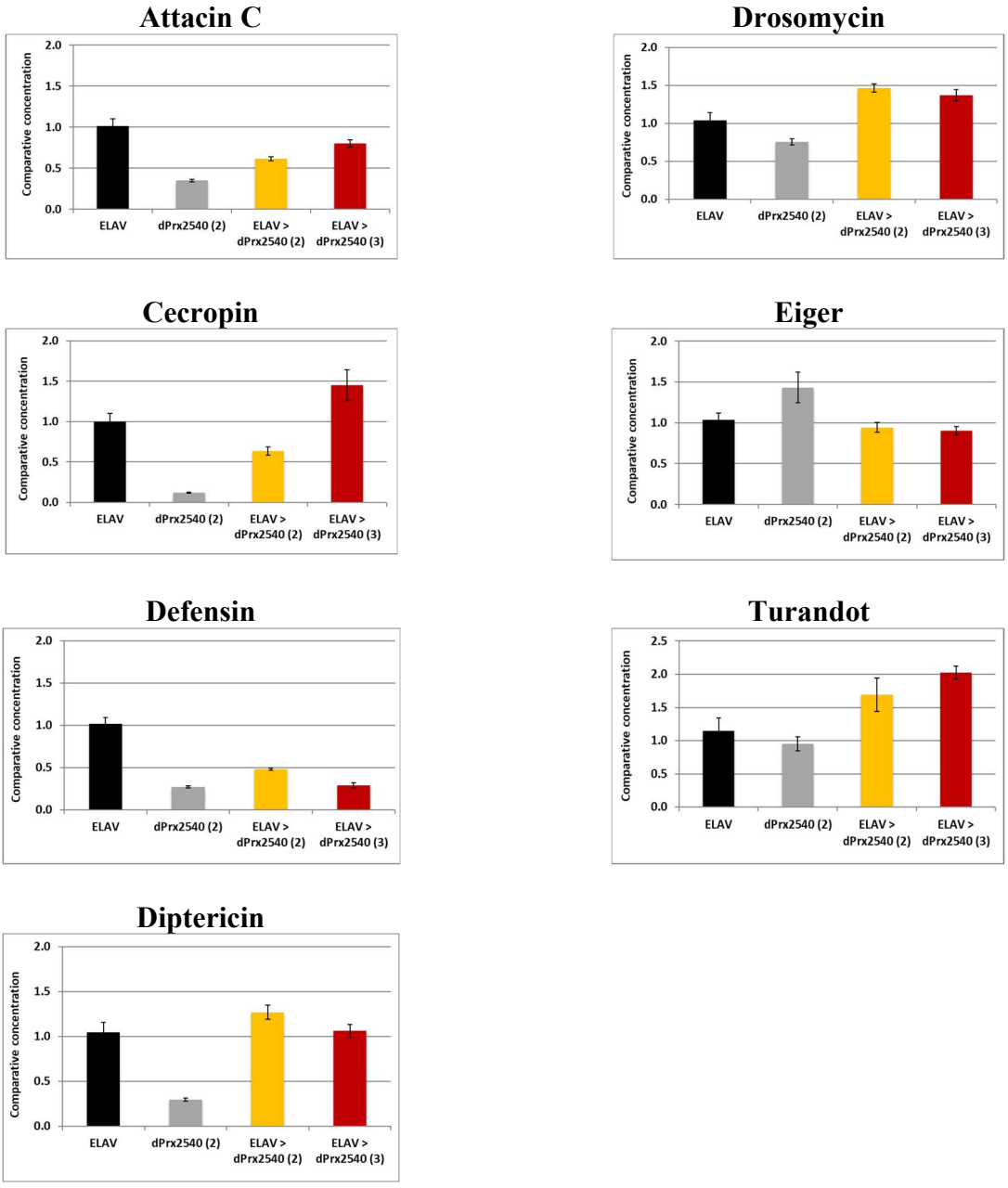

Figure 3.13. Representative AMP expression data from 2x dPrx2540 over-expressors. These graphs indicate the average fold-change in AMP expression relative to ELAV (driver only control) and normalized to RP49 (a housekeeping gene). Expression was measured via qPCR. Error bars indicate standard deviation between three technical replicates. The experiment was performed with 10-day old male flies raised at 28ºC.

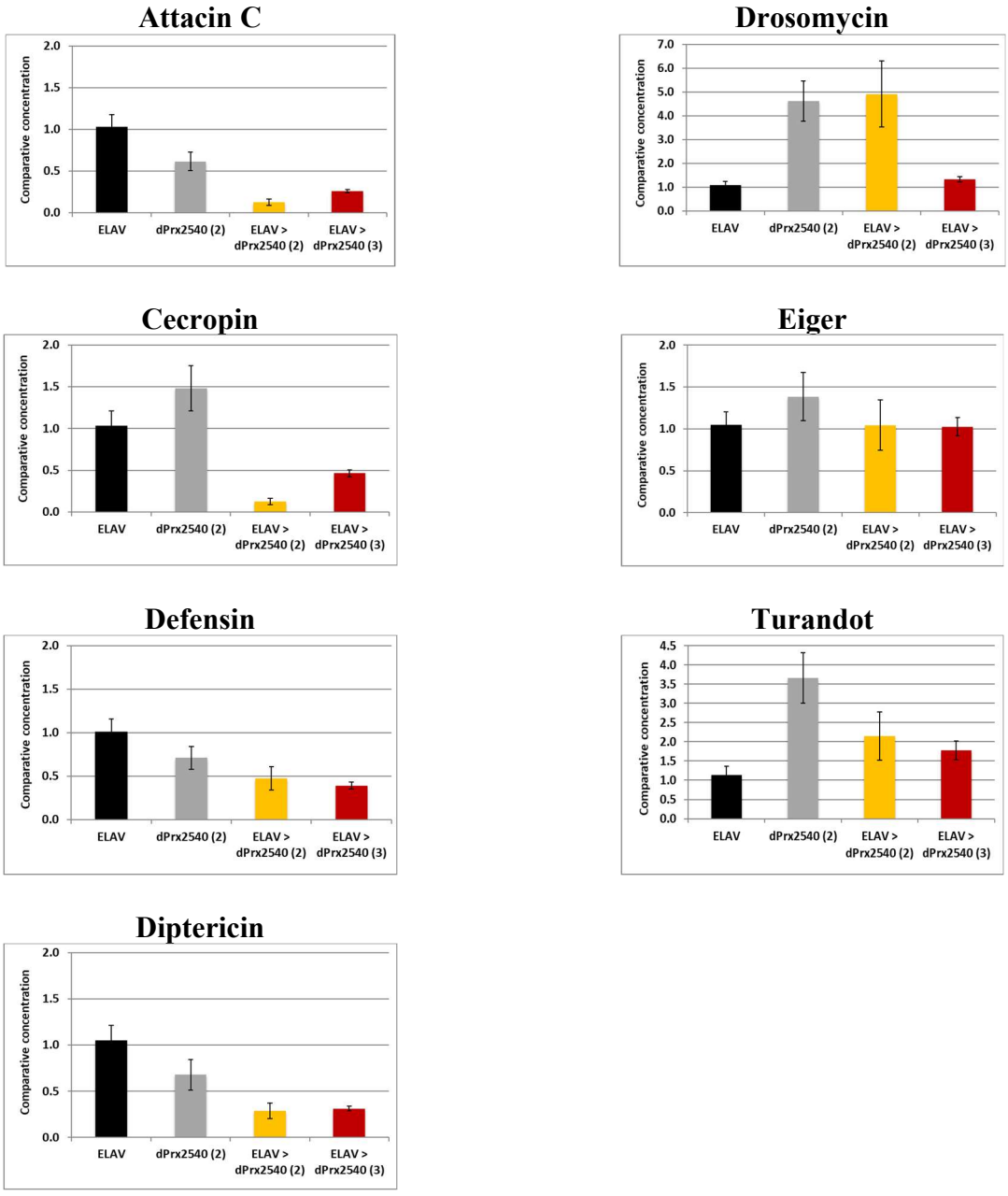

Figure 3.14. Representative AMP expression data from 2x dPrx2540 over-expressors. These graphs indicate the average fold-change in AMP expression relative to ELAV (driver only control) and normalized to RP49 (a housekeeping gene). Expression was measured via qPCR. Error bars indicate standard deviation between three technical replicates. The experiment was performed with 10-day old female flies raised at 28ºC.

The flies tested in this experiment had a single copy of the driver and transgenes, generated in the same manner as those used for the lifespan experiments shown in Figures 3.9 and 3.10. The UAS-Aβ33773 construct is located on the 2nd chromosome. Expression of $A\beta_{42}$ from this construct did not induce the dramatic increase in AMP expression that would be indicative of inflammation (Figure 3.15). The UAS-Aβ33774 construct is located on the 3rd chromosome and, again, expression of $A\beta_{42}$ did not produce an increase in AMP expression (Figure 3.16). Together, these data strongly suggest that expression of human $A\beta_{42}$ alone, in neurons, does not induce neuroinflammation in *Drosophila*.

ELAV > dPrx2540 + Aβ33773 was included to examine possible effects of dPrx2540 over-expression on any inflammation caused by $A\beta_{42}$ expression. Without inflammation in the AD background, any additional effects caused by over-expression of dPrx2540 were indeterminate. However, the dPrx2540 + Aβ33773 control (no driver) actually seems to induce expression of cecropin and diptericin. ELAV > dPrx2540 + Aβ33773 also induces expression of cecropin and diptericin, but to a lesser degree (Figure 3.15). This effect is not seen with ELAV alone (driver only) or Aβ33773 alone (transgene only). These results were repeated alongside the experiments with ELAV > Aβ33774. AMP expression was then tested in a different recombinant line, ELAV > dPrx2540 + Aβ33774, to determine if this effect was common to flies carrying transgenes for dPrx2540 and $A\beta_{42}$ (Figure 3.17). There was no increase in expression for cecropin or diptericin in the ELAV > dPrx2540 + Aβ33774 flies. Therefore, it is possible that the particular recombination event that generated the dPrx2540 + Aβ33773 line disrupted other genes, resulting in elevated expression of cecropin and diptericin. The lifespan of these flies is comparable to other controls such as *yw* and ELAV. Overall, no strong inflammatory response was observed when dPrx2540 and/or arctic $A\beta_{42}$ were expressed in neurons.

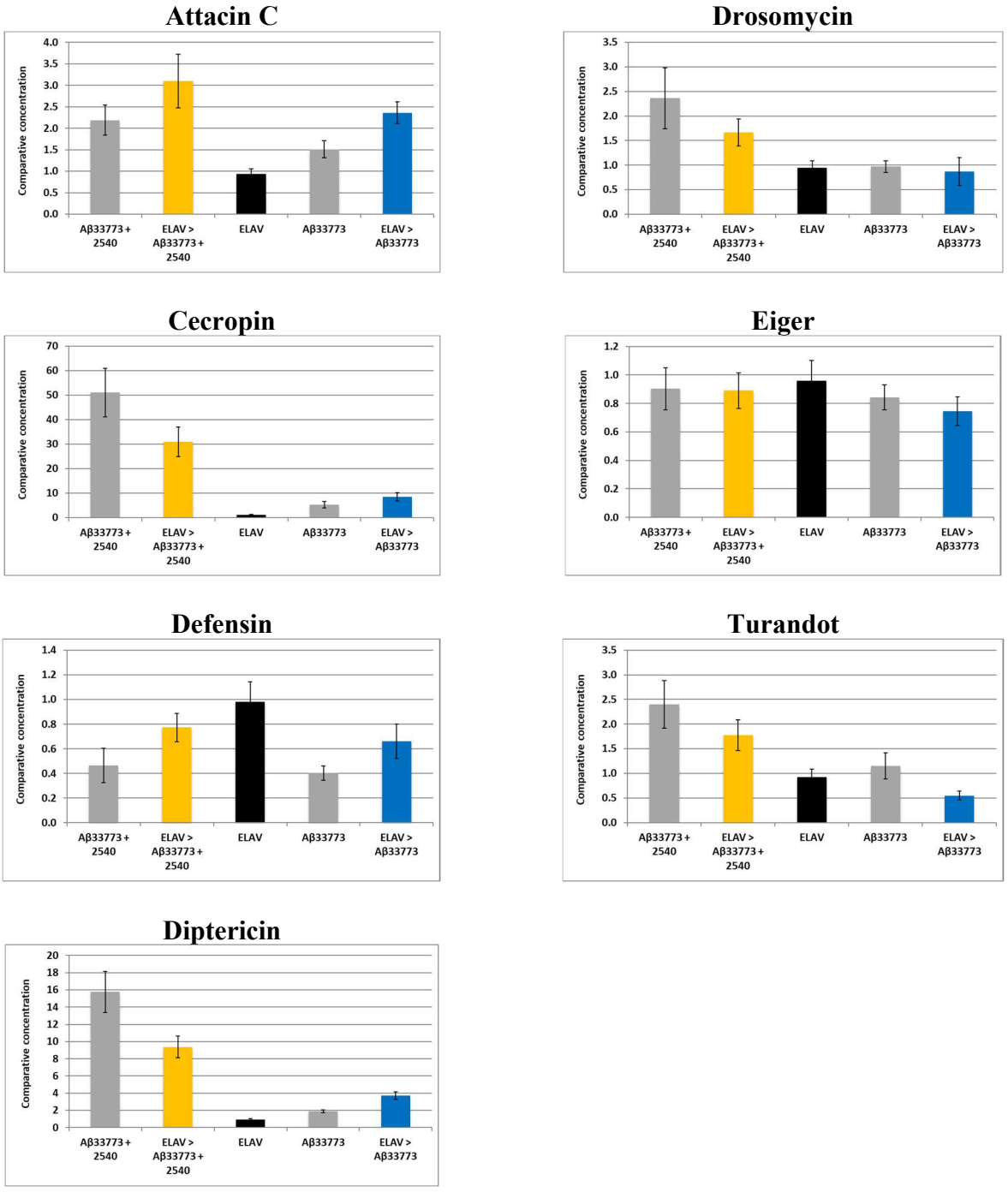

Figure 3.15. Representative AMP expression data from $A\beta_{42}$ expressing flies. These graphs indicate the average fold-change in AMP expression relative to ELAV (driver only control) and normalized to RP49 (a housekeeping gene). Expression was measured via qPCR. Error bars indicate standard deviation between three technical replicates. The experiment was performed with 15-day old male flies raised at 28ºC.

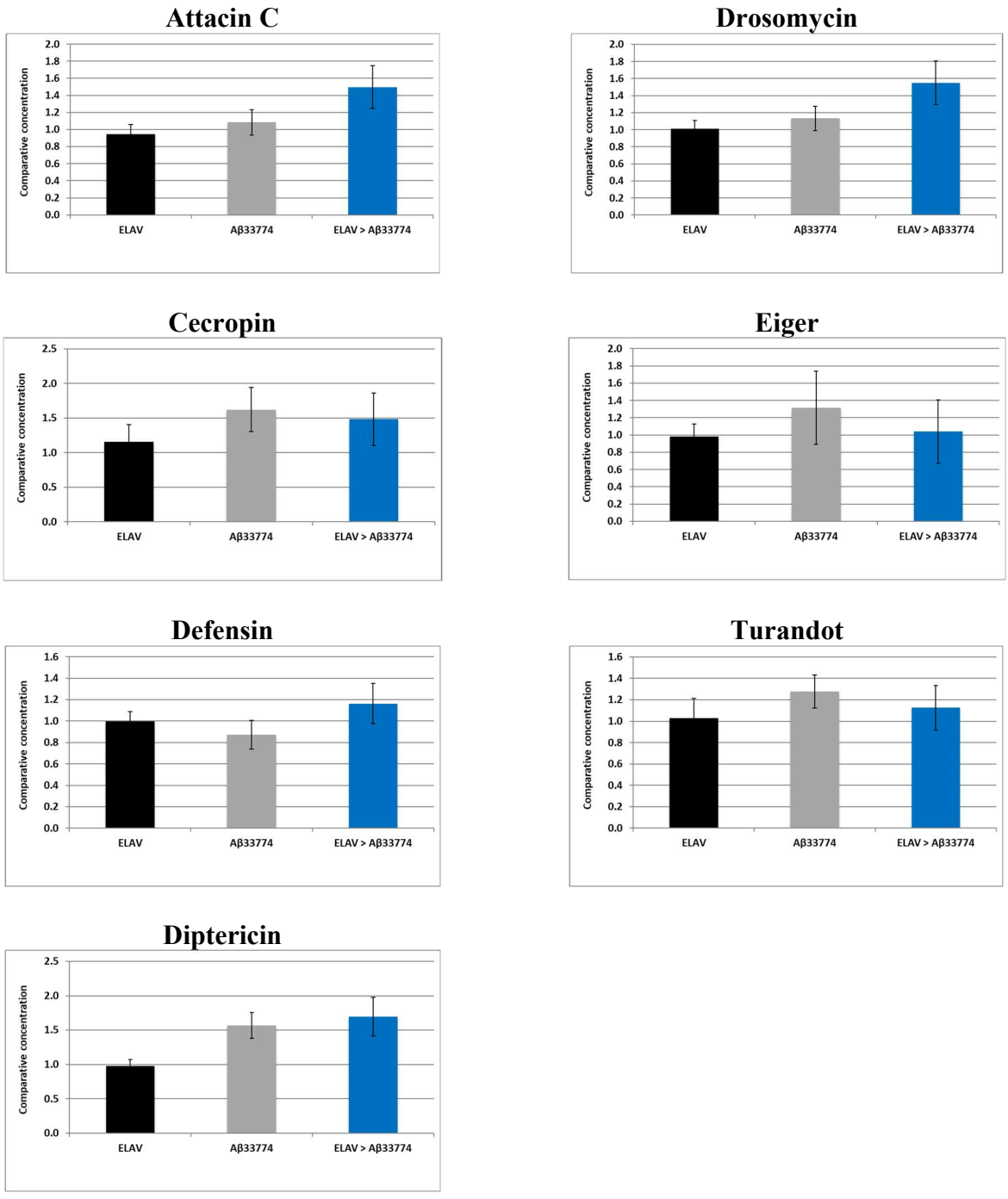

Figure 3.16. Representative AMP expression data from $A\beta_{42}$ expressing flies. These graphs indicate the average fold-change in AMP expression relative to ELAV (driver only control) and normalized to RP49 (a housekeeping gene). Expression was measured via qPCR. Error bars indicate standard deviation between three technical replicates. The experiment was performed with 10-day old male flies raised at 28ºC.

Expression of AMPs in ELAV > Aβ33774 + dPrx2540 (Males)

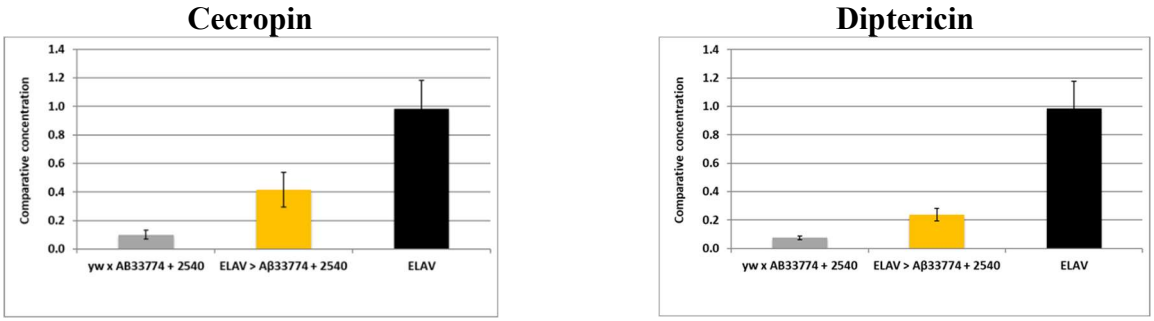

Figure 3.17. AMP expression data from flies expressing Aβ33774 + dPrx2540. These graphs indicate the average fold-change in AMP expression relative to ELAV (driver only control) and normalized to RP49 (a housekeeping gene). Expression was measured via qPCR. Error bars indicate standard deviation between three technical replicates. The experiment was performed with 10-day old male flies raised at 28ºC.

3.4 Mutation of dPrx2540 Active Sites

In order to determine more directly whether PRX or PLA_2 activities of dPrx2540 are responsible for the effects of dPrx2540 expression in the AD background, mutations were made in dPrx2540 to inactivate the appropriate catalytic sites. To ablate PRX activity, the C43S mutation was selected because it was a simple change that leaves a preferred codon for serine. The primer sequence for this mutation is TTACTCCCGTCTCCACCACTGAG, where the underlined "C" is a nucleotide mismatch to generate the point mutation. To ablate PLA_2 activity, the D135A mutation was selected because the mutation would leave a preferred codon for alanine and because mutating either H22 or S28 (of the PLA_2 catalytic triad) would reportedly disrupt other functions of dPrx2540 as well [Fisher, 2018]. The primer sequence for this mutation is CATCAGTCCGGCCCATAAGGTGC, where the underlined "C" is a nucleotide mismatch to generate the point mutation. Reverse compliment primers were made, and the mutagenesis proceeded via primer overlap extension PCR. A double mutant was made by applying the primers for the PLA_2 mutation to the completed PRX mutant. The mutant constructs were ligated into the pUASTattB plasmid used to create the original dPrx2540 over-expressors as discussed in Chapter 2.9. Injection of the mutant constructs into the *yw* background and backcrossing of these flies has been completed. These UAS-dPrx2540(ΔPRX) or (ΔPLA_2) or double (ΔPRX + ΔPLA_2) mutant flies are now being crossed into the 2540null background and into the AD background.

CHAPTER 4

DISCUSSION

Production of arachidonic acid via PLA_2 activity is part of a known pro-inflammatory pathway [Reuters, 2019]. Because Prx6 has PLA_2 function and is upregulated in AD patient brains, it is surmised that this enzyme could exacerbate AD symptoms by helping to drive the neuronal inflammatory response. To test this, dPrx2540 of *Drosophila*, a homolog of human Prx6, was ectopically expressed or suppressed in a *Drosophila* model of AD that expresses human $A\beta_{42}$.

Data from the initial lifespan experiments with dPrx2540 suggests that under-expression of dPrx2540 is beneficial to survival. Surprisingly, over-expression was also mildly beneficial, but the effect was less consistent than with under-expression. Male flies also seemed to have more pronounced benefits than females. The planned lifespan experiments with homozygous over-expressors of dPrx2540 may produce a stronger result that would help with interpretations of data. Both over- and under-expression of dPrx6005 had beneficial longevity effects in females. In males, over-expression of dPrx6005 had no significant impact on longevity whereas under-expression elicited negative effects in terms of early death, but beneficial longevity effects for the remaining flies. However, this survivorship study was only conducted once and will need to be replicated before any conclusions are drawn about this particular protein.

The expression of AMPs as markers of inflammation were measured because dPrx2540 is thought to activate pro-inflammatory pathways via production of arachidonic acid from its PLA_2 activity. If PLA_2 activity is responsible for causing inflammation, then a large increase in dPrx2540 expression would be expected to cause an upregulation in AMPs. However, no significant inflammation was detected from four different dPrx2540 overexpressing lines, in either males or females. With this unexpected result, the question became whether the Drosophila AD lines used in this project experienced neuroinflammation. The lines Aβ33773 and Aβ33774 are known to form Aβ42 plaques and have severely reduced lifespan, indicating that they have an AD phenotype. When tested for inflammation via AMP expression, these AD lines also showed no detectable inflammatory response from fly heads. In *Drosophila*, AMPs are produced in the fat bodies, including one in the head [Imler and Bulet, 2005]. However, *Drosophila* have a glial blood-brain barrier that may prevent direct activity of AMPs in neurons or it may be that protein aggregates, such as AB_{42}, do not stimulate production of AMPs in Drosophila [Schirmeier and Klämbt, 2015]. It is possible that this particular *Drosophila* based model of AD cannot properly simulate an inflammatory response, which may be a limiting factor in this project, but could be valuable information for future studies of AD using *Drosophila* models. Instead, such pathology in neurons may primarily activate glial cells to cleanup protein aggregates and damaged neurons. In fact, glial activation has also been linked to inflammation and AD symptoms and could be measured as an alternative to inflammation in Drosophila [von Bernhardi, 2015]. It is also worth noting that Prx6 was found to be upregulated primarily in glial cells of AD patient brains, so it may be worth over-expressing dPrx2540 with a glial-specific driver such as REPO-Gal4 [Power et al., 2008].

dPrx2540, and mammalian Prx6, may have a complex role in AD. PLA activity could be driving an inflammatory response as predicted, while the PRX activity could be compensating by reducing OS. In the Drosophila AD models used for this study, no significant inflammation was detected in fly heads. Therefore, it is possible that dPrx2540 may not drive inflammation in this model. However, this does not account for the relatively large increase in lifespan seen repeatedly in males in which dPrx2540 expression was reduced by RNAi.

The second major objective of this ongoing project should help with refining interpretations of current data. Currently, most of the major tools required for the second objective have been gathered. Fly lines have been created with all endogenous copies of dPrx2540 removed via CRISPR. Lines have also been generated carrying constructs for the expression of three varieties of mutant dPrx2540: (1) PRX activity ablated, (2) PLA_2 activity ablated, and (3) both PRX and PLA_2 activities ablated. These are currently being crossed with the CRISPR dPrx2540 knockout line to generate recombinant lines which only expresses the desired dPrx2540 mutant genes. These tools will allow very specific testing of the separate effects of each individual function of dPrx2540. If expression of dPrx2540 with PRX activity removed accelerates mortality in the AD background, it might be concluded that PLA_2 activity does indeed exacerbate AD symptoms and that the previously seen beneficial effects of wild type dPrx2540 over-expression were probably the result of PRX activity. If expression dPrx2540 with ablated PRX activity still improves lifespan in the AD background, it might be concluded that the PLA_2 activity of dPrx2540 may actually have a beneficial effect in fly brains. This could be confirmed by a reduction or no change in lifespan in flies expressing only dPrx2540 with PLA_2 activity ablated. This second outcome, though not expected, would not be unreasonable given the reported role of Prx6 in peroxidized membrane repair [Fisher, 2017].

REFERENCES

Addgene. (2019). https://www.addgene.org/vector-database/. Addgene: Vector Database.

Alzheimer's Disease Fact Sheet. (2019). https://www.nia.nih.gov/health/alzheimers-disease-fact-sheet. National Institute on Aging (NIA).

Ahn, J., Jang, K. K., Jo, I., Nurhasni, H., Lim, J. G., Yoo, J.-W., Choi, S. H., and Ha, N.-C. (2018). Crystal structure of peroxiredoxin 3 from Vibrio vulnificus and its implications for scavenging peroxides and nitric oxide. *IUCrJ* 5, 82–92.

Brand, A. H., Manoukian, A. S., Perrimon, N. (1994). Ectopic Expression in Drosophila. *Methods in Cell Biology* 44:635-54.

Castellani, R., Lee, H., Siedlak, S., Nunomura, A., Hayashi, T., Nakamura, M., Zhu, X., Perry,G., and Smith, M. (2009). Reexamining Alzheimer's Disease: Evidence for a Protective Role for Amyloid-β Protein Precursor and Amyloid-β. *Journal Of Alzheimer's Disease* 18, 447-452.

Chen, Z., Zhong, C. (2014). Oxidative stress in Alzheimer's disease. *Neuroscience Bulletin*, 30(20): 271-281.

Crowther, D.C., Kinghorn, K.J., Miranda, E., Page, R., Curry, J.A., Duthie, F.A.I., Gubb, D.C., Lomas, D.A. (2005). Intraneuronal Aβ, non-amyloid aggregates and neurodegeneration in a *Drosophila* model of Alzheimer's disease. *Neuroscience*, 132(1): 123-135.

Dennis, E. A. (1994). Diversity of group types, regulation, and function of phospholipase A2. *Journal of Biological Chemistry* 269, 13057-13060.

Fisher, A. B. (2017) Peroxiredoxin 6 in the repair of peroxidized cell membranes and cell signaling. *Archives of Biochemistry and Biophysics* 617:68-83.

Fisher, A. (2018). The Phospholipase A2 Activity of Peroxiredoxin 6. *Journal of Lipid Research*. 59(7):1132-1147

Govind, S. (2008). Innate immunity in Drosophila: Pathogens and pathways. Insect *Science* 15, 29-43.

Heneka, M., et al. (2015). Neuroinflammation in Alzheimer's disease. *The Lancet Neurology* 14(4):388-405.

Hoover, B., Reed, M., Su, J., Penrod, R., Kotilinek, L., Grant, M., Pitstick, R., Carlson, G., Lanier, L., and Yuan, L. et al. (2010). Tau Mislocalization to Dendritic Spines Mediates Synaptic Dysfunction Independently of Neurodegeneration. *Neuron* 68, 1067-1081.

Imler, J. L., Bulet, P. (2005) Antimicrobial peptides in Drosophila: structures, activities and gene regulation. *Chemical Immunology and Alergy* 86:1-21.

Kim, K., Lee, W., and Kim, E. (2016). Crystal structures of human peroxiredoxin 6 in different oxidation states. *Biochemical And Biophysical Research Communications* 477, 717-722.

Liebthal, M., Maynard, D., and Dietz, K. (2018). Peroxiredoxins and Redox Signaling in Plants. Antioxidants & Redox Signaling 28, 609-624.

Morales, I., Guzman-Martinez, L., Cerda-Troncoso, C., Farias, G., and Maccioni, R. (2014). Neuroinflammation in the pathogenesis of Alzheimer's disease. A rational framework for the search of novel therapeutic approaches. *Frontiers In Cellular Neuroscience* 8.

New England Biolabs. (2019). https://www.neb.com/protocols/0001/01/01/dna-ligation-with-t4-dna-ligase-m0202. Ligation Protocol with T4 DNA Ligase (M0202) | NEB.

Nicolas, J., Lin, Y., Lambeau, G., Ghomashchi, F., Lazdunski, M., and Gelb, M. (1997). Localization of Structural Elements of Bee Venom Phospholipase A2Involved in N-type Receptor Binding and Neurotoxicity. *Journal Of Biological Chemistry* 272, 7173-7181.

Odnokoz, O., Nakatsuka, K., Klichko, V., Nguyen, J., Solis, L., Ostling, K., Badinloo, M., Orr, W., and Radyuk, S. (2017). Mitochondrial peroxiredoxins are essential in regulating the relationship between Drosophila immunity and aging. *Biochimica Et Biophysica Acta (BBA) - Molecular Basis Of Disease* 1863, 68-80.

Power, J., Asad, S., Chataway, T., Chegini, F., Manavis, J., Temlett, J., Jensen, P., Blumbergs, P., and Gai, W. (2008). Peroxiredoxin 6 in human brain: molecular forms, cellular distribution and association with Alzheimer's disease pathology. *Acta Neuropathologica* 115, 611-622.

Prüßing, K., Voigt, A., and Schulz, J. (2013). Drosophila melanogaster as a model organism for Alzheimer's disease. *Molecular Neurodegeneration* 8, 35.

Radyuk, S., and Orr, W. (2018). The Multifaceted Impact of Peroxiredoxins on Aging and Disease. *Antioxidants & Redox Signaling* 29, 1293-1311.

Reuters, T. (2019). Prostaglandin 2 biosynthesis and metabolism FM. *PathwayMaps.com* http://pathwaymaps.com/maps/894

Saul, M., Emmerich, A., Steinhilber, D., and Suess, B. (2019). Regulation of Eicosanoid Pathways by MicroRNAs. *Frontiers In Pharmacology* 10.

Schirmeier, S., and Klämbt, C. (2015). The Drosophila blood-brain barrier as interface between neurons and hemolymph. *Mechanisms Of Development* 138, 50-55.

Sorokina, E., Feinstein, S., Milovanova, T., and Fisher, A. (2009). Identification of the amino acid sequence that targets peroxiredoxin 6 to lysosome-like structures of lung epithelial cells. *American Journal Of Physiology-Lung Cellular And Molecular Physiology* 297, L871-L880.

Thurmond J, Goodman JL, Strelets VB, Attrill H, Gramates LS, Marygold SJ, Matthews BB, Millburn G, Antonazzo G, Trovisco V, Kaufman TC, Calvi BR and the FlyBase Consortium. (2019) FlyBase 2.0: the next generation. *Nucleic Acids Res*. 47(D1) D759–D765

von Bernhardi, R., Eugenín-von Bernhardi, L., and Eugenín, J. (2015). Microglial cell dysregulation in brain aging and neurodegeneration. *Frontiers In Aging Neuroscience 7.*

Wu, Y., and Zhou, B. (2010). TNF-α/NF-κB/Snail pathway in cancer cell migration and invasion. *British Journal Of Cancer* 102, 639-644.

Yun, H., Jin, P., Han, J., Lee, M., Han, S., Oh, K., Hong, S., Jung, E., and Hong, J. (2013). Acceleration of the Development of Alzheimer's Disease in Amyloid Beta-Infused Peroxiredoxin 6 Over-expression Transgenic Mice. *Molecular Neurobiology* 48, 941-951.